

**The Chemical Evolution of the Galaxy:
the two-infall model**

C. Chiappini^{1,2}, F. Matteucci¹

Dipartimento di Astronomia, Università di Trieste, SISSA, Via Beirut 2-4, I-34013 Trieste,
Italy

Instituto Astronômico e Geofísico, Universidade de São Paulo, São Paulo, Brazil

and

R. Gratton³

Osservatorio Astronomico di Padova, Vicolo dell'Osservatorio 5, 35100, Padova, Italy

Received _____; accepted _____

Accepted for publication in *Astrophysical Journal*

ABSTRACT

In this paper we present a new chemical evolution model for the Galaxy which assumes two main infall episodes for the formation of halo-thick disk and thin disk, respectively. We do not try to take into account explicitly the evolution of the halo since our model is better suited for computing the evolution of the disk (thick plus thin) but we implicitly assume that the timescale for the formation of the halo was of the same order as the timescale for the formation of the thick disk.

The formation of the thin-disk is much longer than that of the thick disk, implying that the infalling gas forming the thin-disk comes not only from the thick disk but mainly from the intergalactic medium.

The timescale for the formation of the thin-disk is assumed to be a function of the galactocentric distance, leading to an inside-out picture for the Galaxy building. The model takes into account the most up to date nucleosynthesis prescriptions and adopts a threshold in the star formation process which naturally produces a hiatus in the star formation rate at the end of the thick disk phase, as suggested by recent observations. The model results are compared with an extended set of observational constraints both for the solar neighbourhood and the whole disk. Among these constraints, the tightest one is the metallicity distribution of the G-dwarf stars for which new data are now available. Our model fits very well these new data.

The model predicts also the evolution of the gas mass, the star formation rate, the supernova rates and the abundances of 16 chemical elements as functions of time and galactocentric distance. We show that in order to reproduce most of these constraints a timescale ≤ 1 Gyr for the (halo)-thick-disk and of 8 Gyr for the thin-disk formation in the solar vicinity are required.

We predict that the radial abundance gradients in the inner regions of the disk ($R < R_{\odot}$) are steeper than in the outer regions, a result confirmed by recent abundance determinations, and that the inner ones steepen in time during the Galactic lifetime. The importance and the advantages of assuming a threshold gas density for the onset of the star formation process is discussed.

1. Introduction

The study of chemical evolution of our Galaxy has been addressed by several models in recent years. Generally, a good agreement between model predictions and observed properties of the Galaxy is obtained by models which assume that the disk formed by infalling gas, as suggested in the pioneering work of Chiosi (1980). Very different models assuming gas accretion onto the Galactic disk were constructed such as, for instance, viscous models (Lacey and Fall 1985, Sommer-Larsen and Yoshii 1989, 1990, Tsujimoto et al. 1995), inhomogeneous models (Malinie et al. 1993), detailed chemical evolution models (Matteucci and Greggio 1986, Tosi 1988, Matteucci and François 1989 (MF89), Pagel 1989, Matteucci and François 1992, Carigi 1994, Giovagnoli and Tosi 1995, Ferrini et al. 1994, Pardi and Ferrini 1994, Pardi et al. 1995, Prantzos and Aubert 1995, Timmes et al. 1995) and chemodynamical models (Samland and Hensler 1996, Burkert et al. 1992). However, as recently pointed out by Prantzos and Aubert (1995), the model predictions are usually compared with different sets of observables by the different authors and they suggested that a *minimal set* of observables should be adopted.

It is also of fundamental importance to relax the instantaneous recycling approximation (IRA) and to account for the contribution of type Ia supernovae (SNe). This allows us to make a correct comparison between models and observational data, especially because the observed metallicity is usually represented by the iron abundance.

Recently, Tosi (1996 and references therein) compared different models (without dynamics) for the chemical evolution of the Galactic disk where IRA was relaxed. She showed that, in spite of the fact that these models were based on very different assumptions, they all could fit a reasonable number of the solar neighbourhood constraints, whereas significant differences were present in the predictions for the radial distributions of the various quantities as well as in the history of radial abundance gradients. These facts

suggest that new models should be tested on the observed radial properties of the disk. With respect to the available observational constraints, the last years have been of crucial importance. New data are now available concerning the age-metallicity relation, the G-dwarf metallicity distribution, the relative abundances of α -elements and iron and the radial abundance gradients and they require the construction of new models. In particular, in a recent paper Gratton et al. (1996) showed that the distribution of the abundances of α -elements to Fe for a large homogeneous sample of stars in the solar neighbourhood seems to indicate a short timescale for the evolution of the halo and thick disk phases and a sudden decrease in the star formation in the epoch preceding the formation of the thin disk. They identified three kinematically distinct populations: i) a population made of halo, thick-disk and perhaps bulge stars originating from the dissipative collapse of the halo, ii) a population of thin disk stars originating from the even more dissipative collapse of the disk, and finally iii) a population of thick-disk stars the origin of which should be different from the others, namely they should have formed in satellite galaxies and then accreted by the Galaxy during the star formation gap. This last component should contribute negligibly to the total number of stars but it should represent $\sim 50\%$ of the stars with $[\text{Fe}/\text{H}] < -1.0$.

An analogous result was already found by Beers and Sommer-Larsen (1995). These authors have shown that the thick disk population extends to very low metallicities. For instance, according to that work about 30% of metal-deficient stars in their sample, with metallicities $[\text{Fe}/\text{H}] \leq 1.5$, have kinematic properties which are typical of a thick disk population. This metal-weak tail of the thick disk population could have its origin in a major accretion episode during the Galaxy evolution (Beers and Sommer-Larsen 1995 and references therein). This is a very important new information which induces to consider a different picture of Galaxy formation than those previously adopted.

Previous models, in fact, (MF89 and Matteucci and François, 1992) were based on only

one episode of infall during which first formed the halo and then the disk or (Pardi et al. 1995) were assuming that halo, thick and thin disk formed simultaneously but at different rates (pure collapse picture). These models, however, are difficult to conciliate with the new results discussed above.

In this paper we present a new chemical evolution model for the Galaxy which assumes two main infall episodes. The first one is responsible for the formation of the population i) namely, the one made of that fraction of the halo and thick disk stars which originated from a fast dissipative collapse such as that suggested by Eggen et al. (1962). It is beyond the scope of the present work to describe explicitly the evolution of the halo as we are using a formalism based on surface densities which is suitable for disk models. This phase, however, is included implicitly in our thick-disk phase by assuming that the timescale for the formation of the internal halo was of the same order than the timescale for the formation of the thick disk (Gratton et al. 1996). The second infall episode forms the thin disk component with a timescale much longer than that of the thick disk formation. This model implies that most of the galactic thin disk, if not all, was formed out of accreted extragalactic material.

This scenario for the Galaxy formation is not only in agreement with the results of Gratton et al. (1996) and Beers and Sommer-Larsen (1995) but also with the works by Wyse and Gilmore (1992) and Ibata and Gilmore (1995). In fact, these last papers have shown that the spheroidal (bulge and halo) and disk (thick and thin disks) components of our Galaxy have substantial different angular momentum distributions. This fact strongly suggests that the previously adopted picture, where the gas shed from the halo was the main contributor to the thin disk formation, should be revised (Pagel and Tautvaisiene 1995).

The aim of this paper is to test the two infall chemical evolution model with respect to

the maximum number of available observational constraints in the Galaxy. Relatively to our previous models this one adopts the most recent nucleosynthesis prescriptions published by Woosley and Weaver (1995) for the elements produced in massive stars, and by Dearborn et al. (1995) for ${}^3\text{He}$ and D abundances. The inclusion of a threshold in the gas density below which the star formation process stops, makes the model more physical and produces new important effects.

In section 2 we describe the set of observational constraints to be compared with the models. In section 3 we present the model assumptions, the nucleosynthesis prescriptions and the adopted input parameters. In section 4 we compare the model predictions with the observed properties. Section 5 presents the conclusions.

2. Observational Constraints

A good model of chemical evolution of the Galaxy should reproduce a number of constraints which is greater than the number of free parameters. Therefore, it is very important to choose a high quality set of observational data to be compared with models predictions. Our set of constraints include:

- The relative number of thin disk and metal-poor stars (halo plus part of thick disk stars) in the solar cylinder
- Type I and type II supernova rates at the present time
- Solar abundances
- Present-day gas fraction
- Age-Metallicity relation

- Present-day infall rate
- Metallicity distributions for disk and metal-poor stars
- The variation in the relative abundances of the most common chemical elements
- Radial profiles for the SFR and gas mass density
- Radial abundance gradients

2.1. Solar abundances

The solar abundances should represent the chemical composition of the interstellar medium in the solar neighbourhood at the time of sun formation (4.5 Gyrs ago). However, Cunha and Lambert (1992) showed that the abundance of oxygen in the Orion nebula is smaller by a factor of 2 than the solar one (Anders and Grevesse 1989), at variance with the increase of the metal abundances in the Galaxy with time as predicted by the chemical evolution models. Thus, it is not clear whether the solar composition should be considered as representative of the local ISM 4.5 Gyrs ago, a possibility being that the sun was born in a region closer to the Galactic center and then moved to the present region. It should also be noted that the elemental abundances are uncertain. As discussed by Timmes et al. (1995), given the uncertainties involved, abundance values falling within a factor of two inside the observed ones can be considered as being in agreement with the solar data.

2.2. Age-metallicity relation

For the age-metallicity relation in the solar neighbourhood the most recent data were derived by Edvardsson et al. (1993) from F stars with $7.7 < R < 9.3$, where R is the galactocentric distance corresponding to the star birth places. These authors present a

spectroscopically calibrated age-metallicity relationship which constitutes the most accurate data set available at present. Previous data were based on photometric surveys (Twarog 1980, Carlberg et al. 1985, Meusinger et al. 1991) which did not contain kinematic information. However, this more accurate age-metallicity relation obtained by Edvardsson et al. (1993) shows a considerable scatter at almost all ages and hence any chemical evolution models can easily reproduce this relationship which does not constitute a tight constraint anymore (figure 1a and 1b).

The observed scatter in these data could be real as discussed by François and Matteucci (1993) and Matteucci (1994), and it could be the consequence of the overlapping of different stellar populations observed in the solar vicinity, possibly caused by orbital diffusion. Other explanations are given in Edvardsson et al. (1993) (see also Pagel and Tautvaisiene 1995 and references therein).

2.3. Stellar metallicity distribution

An important constraint on chemical evolution models is the metallicity distribution of G-dwarfs for the solar vicinity. The G-dwarf metallicity distribution is representative of the chemical enrichment of the Galaxy, since these stars have lifetimes greater than or equal to the age of the Galaxy and hence can provide a complete record of the chemical evolutionary history. Until now, all the authors made use of the G-dwarf metallicity distribution published by Pagel and Patchett (1975) and revised by Pagel (1989) and Sommer-Larsen (1991). Recently, two different groups using new observations and up to date techniques, published new data on the G-dwarf distribution (Rocha-Pinto and Maciel 1996, Wyse and Gilmore 1995). The basic differences are in the new adopted catalog, namely, the Third Gliese Catalog, and in the calibration used to determine the metallicity. This calibration is based on Strömberg photometry which allows a more reliable estimation of the metallicity

than does the one based on UBV photometric system as in Pagel and Patchett (1975). As can be seen in figure 2, these new data are very similar to each other but very different from the previous ones. In particular, the new data show a well-defined peak in metallicity (between $[\text{Fe}/\text{H}]=-0.3$ and $0.$), which was not evident in the previous data.

2.4. Relative abundances

Another important constraint is the behaviour of the α -to-iron ratio as a function of iron. While the α -elements (O, Ne, Mg, Si, Ca etc..) are produced only by type II SNe (which have high mass progenitors with short life time), most of the iron is produced by type Ia SNe, which are believed to be the result of the explosion of C-O white dwarfs in binary systems. Iron release from type Ia SNe begins not before several 10^7 years after the birth of a star generation, and the bulk of restitution takes up to some Gyrs, depending on the assumptions on the binary system characteristics, explosion mechanism and star formation rate (SFR). Therefore, the delayed arrival of the iron produced by type Ia SNe is responsible for the observed decrease in the $[\alpha/\text{Fe}]$ ratio as a function of the iron abundance in the solar vicinity (Greggio and Renzini 1983, Matteucci and Greggio 1986, MF89). Recently Gratton et al. (1996) obtained an uniform data set for iron and oxygen abundances in field stars based on the original equivalent widths reported in a serie of papers (Gratton and Sneden 1991, Gratton and Sneden 1994, Tomkin et al. 1992, Sneden et al. 1991, Kraft et al. 1992, Nissen and Edvardsson 1992, Zhao and Magain 1990). In total, the authors determined $[\text{O}/\text{Fe}]$ ratios for about 160 stars. These data are presented in figure 3. Such abundances constitute an important constraint to the chemical evolution models. As shown in Gratton et al. (1996), a plot of $[\text{Fe}/\text{O}]$ vs. $[\text{O}/\text{H}]$ shows that $[\text{Fe}/\text{O}]$ increases by $\simeq 0.2$ dex while the $[\text{O}/\text{H}]$ ratio holds constant during the transition from the thick to the thin disk phase. This clearly indicates the existence of a gap in the star formation

rate during the transition between these two phases. In this work we also compare the model predictions for the abundance ratios of other elements with respect to iron with the available observations (section 4).

2.5. Abundance gradients

The existence of abundance gradients in the Galaxy (and in the disk of external galaxies) has been one of the fundamental constraints for chemical evolution models. Observations of H II regions (Shaver et al. 1983) and planetary nebulae of type II, which can be considered tracers of the abundance gradients in the ISM (Maciel and Köppen 1994, Maciel and Chiappini 1994), show a negative abundance gradient for oxygen of the order of -0.07 dex/kpc. Planetary nebulae also show gradients for other elements such as Ne, Ar and S, in the galactocentric range 5-12 kpc, similar to that of oxygen. All previous chemical evolution models tried to reproduce this feature. However, at present, the existence of such abundance gradients is controversial. Recently Kaufer et al. (1994) obtained spectra and abundances of B-type main sequence stars in young open clusters and in H II regions, in the galactocentric distance range 7-16 kpc and they found a flat gradient for O and N in this region. The authors stressed that early type B stars on or near the main sequence should be good indicators for the present composition of the interstellar medium since they have the advantage of being still located near their birthplace, they did not underwent through mixing processes and are bright enough to be observed at great distances. Based on these data, they concluded that there is no gradient at least for $R > 6$ kpc, where R is the galactocentric distance. As suggested by the authors, this apparent controversial result of gaseous nebulae and B stars on radial abundance gradients could be solved if the data of Shaver et al. (and also those on PNe) are interpreted as showing a gradient only in the inner Galaxy ($R < R_{\odot}$) and a flat profile at larger distances. This was also suggested

by Vilchez and Esteban (1996), who studied the chemical composition of H II regions at larger radii and, despite the scatter, he also found a flat oxygen gradient for galactocentric distances greater than that of the sun. Recently, a result reported by Simpson et al. (1995), based on infrared abundance measurements in H II regions, also shows that the radial abundance gradients seem to be different in the outer and inner parts of the Galaxy. On the other side, recent work by Liu et al. (1995) shows that the *standard* method of abundance determination in gaseous nebulae, based on forbidden-line analysis, may underestimate the abundances by a factor of two to three. How this can affect the abundance gradients obtained from gaseous nebulae is still not clear. Given these controversial results, the observed abundance gradients should be considered with caution.

The observational values for the other constraints in the solar neighbourhood, namely the relative number of thin-disk and metal poor stars, the supernova rates at the present time, the present day gas fraction, the solar abundances, the enrichment of helium relative to metals during the Galactic lifetime ($\Delta Y/\Delta Z$), the present time star formation and infall rates are shown in tables 2 and 3 together with the model results (section 4).

3. The Model

3.1. Model Assumptions

Our model is based on the MF89 model, but the (halo)-thick-disk and thin disk evolutions occur at different rates due mostly to different accretion rates. As in the MF89 model the Galactic disk is approximated by several independent rings, 2 kpc wide, without exchange of matter between them. The basic equations are the same as in MF89:

$$\begin{aligned}
 \frac{d G_i(r, t)}{dt} = & - X_i(r, t) \Psi(r, t) + \int_{M_L}^{M_{Bm}} \Psi(r, t - \tau_M) (Q_M)_i \Phi(M) dM + \\
 & A \int_{M_{Bm}}^{M_{BM}} \Phi(M_B) \left[\int_{\mu_m}^{0.5} f(\mu) \Psi(r, t - \tau_{M2}) (Q_{M1})_i(t - \tau_{M2}) d\mu \right] dM_B \\
 & + (1 - A) \int_{M_{Bm}}^{M_{BM}} \Psi(r, t - \tau_{MB}) (Q_{MB})_i(t - \tau_{MB}) \Phi(M_B) dM_B \\
 & + \int_{M_{BM}}^{M_U} \Psi(r, t - \tau_M) (Q_M)_i(t - \tau_M) \Phi(M) dM + (X_i)_{inf} \frac{d G(r, t)_{inf}}{dt} \quad (1)
 \end{aligned}$$

where $G_i(r, t) = [\sigma_g(r, t) X_i(r, t)]/\sigma(r, t_G)$ with $G_i(r, t)$ being the normalized surface gas density in the form of the element i , $\sigma(r, t_G)$ being the present time total surface mass density, $\sigma_g(r, t)$ the surface gas density and $X_i(r, t)$ the abundance by mass of an element i . For a detailed description of the meaning of each symbol in equation (1) see Matteucci and Greggio (1986). The two main differences between the present model and the MF89 model are the rate of mass accretion and the rate of star formation. This model assumes two distinct infall episodes: the first during which the thick disk is formed and the second, delayed relatively to the first, during which the thin disk forms. The reader should keep in mind that in this work we do not try to model explicitly the galactic halo and that the halo evolution (i.e. very low metallicity stars) is included in the evolution of the thick disk (see section 1). The thin disk starts forming roughly at the end of the thick disk phase. In this model, the material accreted by the Galactic thin disk comes mainly from extragalactic sources and this is the fundamental difference between our present model and the one by MF89. The extragalactic sources could be, for instance, the Magellanic Stream or a major accretion episode (see Beers and Sommer-Larsen and references therein). A long timescale for the formation of the disk was also suggested by chemodynamical models (Burkert et al. 1992) which predict a delay of several billion years between the formation of the last stars in the halo and the appearance of a disk.

The new expression for the rate of mass accretion in each shell is given by:

$$\frac{d G_i(r, t)_{\text{inf}}}{dt} = \frac{A(r)}{\sigma(r, t_G)} (X_i)_{\text{inf}} e^{-t/\tau_T} + \frac{B(r)}{\sigma(r, t_G)} (X_i)_{\text{inf}} e^{-(t-t_{\text{max}})/\tau_D} \quad (2)$$

where $G_i(r, t)_{\text{inf}}$ is the normalized surface gas density of the infalling material in the form of the element i , $(X_i)_{\text{inf}}$ gives the composition of the infalling gas, which we assume to be primordial, t_{max} is the time of maximum gas accretion onto the disk, and τ_T and τ_D are the timescales for the mass accretion in the thick disk and thin disk components, respectively. These are the two really free parameters of our model and are constrained mainly by comparison with the observed metallicity distribution in the solar vicinity. The t_{max} value is chosen to be 2 Gyrs and roughly corresponds to the end of the thick disk phase. The quantities $A(r)$ and $B(r)$ are derived by the condition of reproducing the current total surface mass density distribution in the solar neighbourhood. The current total surface mass distribution is taken from Rana (1991). For the thin disk we assume a radially varying $\tau_D(r)$ which implies that the inner parts of the thin disk are built much more rapidly than the outer ones. In other words, we are dealing with an inside-out picture, as suggested by previous models (Larson 1976, MF89, Burkert et al. 1992). According to Burkert et al. (1992) the reason for an inside out picture of the disk formation is the strong dependence of the disk evolution on its surface density which is higher at inner regions, whereas the reason proposed by Larson (1976) was an infall timescale which increases with the galactocentric distance.

The adopted radial dependence of τ_D is:

$$\tau_D(r) = 0.875r - 0.75 \quad (3)$$

The expression (3) was built in order to obtain a timescale for the bulge formation ($R < 2$ kpc) of 1 Gyr, in agreement with the results of Matteucci and Brocato (1990), and a timescale of 8 Gyr at the solar neighbourhood, which best reproduces the G-dwarf

metallicity distribution (we are adopting $R_\odot = 10$ kpc). We assume also that the e-folding time of the thick disk infall rate is $\tau_T = 1$ Gyr, which roughly coincides with the appearance of the first type Ia SNe and which leads to a good agreement with the available constraints (section 4).

For the star formation rate we adopt the same expression as in MF89, which has the same functional form for both thick and thin disk phases:

$$\Psi(r, t) = \tilde{\nu} \left[\frac{\sigma(r, t)}{\tilde{\sigma}(\tilde{r}, t)} \right]^{2(k-1)} \left[\frac{\sigma(r, t_G)}{\sigma(r, t)} \right]^{(k-1)} G^k(r, t)$$

$$\Psi(r, t) = 0. \quad \text{when } \sigma_g(r, t) \leq 7M_\odot pc^{-2}. \quad (4)$$

where $\tilde{\nu}$ is the efficiency of the star formation rate expressed in units of Gyr^{-1} , $\tilde{\sigma}(\tilde{r}, t)$ is the total surface mass density at a particular distance \tilde{r} from the Galactic center which is taken, as in Chiosi (1980) and MF89, equal to 10 kpc. As it will be discussed in section 4, the k and $\tilde{\nu}$ parameters of the star formation rate are not arbitrarily chosen. For the models to be in agreement with the observational constraints these two parameters must be restricted to a very small range of values (see section 5).

In the majority of chemical evolution models the star formation rate is assumed to depend on the surface gas density: $\Psi = A \sigma_g^k$, where k varies from 1 to 2 (Kennicutt 1989). According to Dopita and Ryder (1994), both a law of the form of $\Psi = A \sigma_g$, and a star formation dependent on the angular velocity at the radial point considered, e. g., triggered by the spiral arms, seem to be excluded by observations. Instead, they suggest that a star formation which depends either on the surface gas density or on the total surface mass density, similar to the one presented in equation (4), is in better agreement with the observations. Subsequent models have adopted different formulations for the coefficient A and its radial variation. One of them, as proposed originally by Talbot and Arnett (1975)

and adopted by other authors (cf. Chiosi 1980, Dopita 1985, MF89) was a dependence on the total surface mass density. This can be understood as a way to take into account the *local environment* or, in other words, to consider the fact that the more important is the gravitational potential, the easier is for the gas to collapse into stars. The consequences of the adoption of a star formation rate given by equation (4) will be discussed in section 4. This model also considers a star formation threshold of $7M_{\odot}pc^{-2}$ (Gratton et al. 1996 and references therein), which means that below a critical surface gas density there is no star formation. This threshold is suggested by observations relative to the massive star formation in external galaxies (Kennicutt 1989). The physical reason for a threshold in the star formation is related to the gravitational stability according to which, below a critical density the gas is stable against density condensations, and consequently the star formation is suppressed, the actual critical value depending also on the rotational properties of the galaxy. The resulting star formation rate is shown in figure 4, for model A, where the threshold effect is clear during the thick disk phase and also at the end of the thin disk evolution.

As in MF89 the adopted initial mass function (Scalo 1986) is assumed to be constant in space and time.

The input parameters (ν_T , ν_D , k_T , k_D , τ_T , τ_D) are summarized in Table 1 where model A corresponds to our best model. The subscripts T and D refer to the thick and thin disk, respectively. All the models listed in Table 1 have the same threshold in the star formation rate. The model predicts the abundances of the elements H, D, 3He , 4He , C, O, N, Ne, Mg, S, Si, Ca, Fe, Zn, Cu, n-rich elements, the gas density, total mass density, star density, rate of type I and type II SNe as functions of time and galactocentric distance.

3.2. Nucleosynthesis Prescriptions

One of the most important ingredients for chemical evolution models is the nucleosynthesis prescription and the computation of stellar yields. As in MF89, we adopted the Talbot and Arnett (1975) formalism.

For the D and ${}^3\text{He}$ nucleosynthesis we adopted very recent results taken from Dearborn et al. (1995). The authors have computed new stellar models which give the production and destruction of ${}^3\text{He}$ and D , for stellar masses in the range of 0.65 to $100 M_{\odot}$. They tried several non-standard models in order to overcome the problem of the excessively large ${}^3\text{He}$ production in low and intermediate mass stars which leads to an overabundance of such element in the interstellar medium, as predicted by almost all the available chemical evolution models (Tosi 1996). In the present work we adopted one of such prescriptions, characterized by the following values of $6.2 \cdot 10^{-5}$ and $3.5 \cdot 10^{-5}$ for the primordial abundances by mass of D and ${}^3\text{He}$, respectively, and $2.1 \cdot 10^{-5}$ for the main sequence ${}^3\text{He}$ abundance.

For Zn and Cu we adopted the prescriptions given by the best model of Matteucci et al. (1993).

3.2.1. *Low and Intermediate Mass Stars: ($0.8 \leq M/M_{\odot} \leq 8$)*

Single Stars : The single stars in this mass range contribute to the Galactic enrichment through planetary nebula ejection and quiescent mass loss. They enrich the interstellar medium mainly in He, C and N. For these stars, which end their lives as white dwarfs, we adopt the prescriptions of Renzini and Voli (1981), for the case $\alpha = 1.5$ and $\eta = 0.33$. More recent calculations for the low and intermediate mass stars contribution have been computed by Marigo et al (1996). These calculations were made for a scenario which considers the overshooting process in which the M_{up} corresponds to $4 M_{\odot}$. In this

work we opted for the stellar evolution scenario without overshooting.

Type Ia SNe: Type Ia SNe are thought to originate from C-deflagration in C-O white dwarfs in binary systems. The type Ia SNe contribute to a substantial amount of iron ($\sim 0.6M_{\odot}$ per event) and to non-negligible quantities of Si and S. They also contribute to other elements such as O, C, Ne, Ca, Mg and Ni, but in negligible amounts when compared with the masses of such elements ejected by type II SNe. The adopted nucleosynthesis prescriptions are from Thielemann et al. (1993) and they are an updated version of those utilized in MF89 (Nomoto et al. 1984). The differences between these new yields and the old ones are mainly for Ne and Mg, but small enough to have no influence on the model predictions. As in MF89, type Ib SN events are assumed to be a half of the total number of type I SN events and to contribute only to the iron abundance ($\sim 0.3M_{\odot}$ per event, MF89).

3.2.2. Massive Stars: ($8 < M/M_{\odot} \leq 100$)

These stars are the progenitors of type II SNe. For this range of masses we adopt up to date stellar evolution calculations by Woosley and Weaver (1995) for the following elements: 4He , ${}^{12}C$, ${}^{13}C$, ${}^{14}N$, ${}^{16}O$, ${}^{20}Ne$, ${}^{24}Mg$, ${}^{28}Si$, ${}^{32}S$, ${}^{40}Ca$ and ${}^{56}Fe$. The major advantage of these new calculations is that explosive nucleosynthesis is taken into account. This was not the case in the yields adopted by MF89 (Woosley and Weaver 1986) relative to pre-supernova models which required a very uncertain correction factor to take into account the fact that part of Si and S is transformed into iron by explosive nucleosynthesis and that part of some elements falls back onto the collapsing core before the explosion starts (MF89). The second advantage is that in the new calculations the yields for ${}^{13}C$ and ${}^{14}N$ are also included. There are important differences between these new prescriptions for the massive nucleosynthesis yields and those previously reported by Woosley and Weaver (1986). In

particular, for the elements He, Ne and Fe the new yields are higher. On the other hand, the new values for Mg, Si, S and Ca are lower than the previous ones (see Gibson 1996 for a comparison between stellar yields from different sources). We present in figure 5 the masses ejected in form of various elements, weighted by the IMF as a function of the initial mass of the progenitor star. Comparing this figure with figure 4 of MF89 we see that the major differences arise in the Si and S abundances for which the explosive nucleosynthesis is very important, as discussed before. The effect of these new yield prescriptions on models predictions will be discussed in section 4.

4. Results

We ran a large number of models for the solar vicinity and the whole disk, varying the star formation rate parameters (i.e. k and ν) and also the timescales for the thick and thin disk formation (i.e. τ_T and τ_D). A positively surprising result is that only very few combinations of such parameters lead to an agreement with the considered set of observational constraints. Table 2 presents the results of the models of table 1 compared with the current observational quantities, for the solar vicinity. We remind that model A is our best model.

4.1. The relative number of metal poor and metal rich stars

As discussed by Matteucci et al. (1990) and references therein, attempts to form a disk out of already enriched halo gas and with an initial mass function constant in space and time overestimate the fraction of halo stars, although these models reproduce the distribution of the G-dwarfs (MF89). It was then suggested that infall of primordial extragalactic gas coupled with infall of halo gas could overcome this problem. It is clear

from our models that in order to obtain a reasonable number of metal poor stars and simultaneously fit the metallicity distribution of the solar vicinity is necessary to decouple the evolution of the (halo)-thick-disk from that of the thin disk. As already pointed out in section 1, this decouplement is also required from the observational point of view (Wyse and Gilmore 1992, Beers and Sommer-Larsen 1995).

The observed value of the relative number of disk and halo stars suggested by Pagel and Patchett (1975) is 3 %. However, this value is underestimated as it is based on stars observed only up to a certain scale height above the Galactic plane ($\simeq 1 \text{ kpc}$ for G-dwarf stars). Matteucci et al. (1990) estimated that the number of stars contained in a cylinder around the solar neighbourhood with practically an infinite height above the Galactic plane, which is the actual quantity predicted by the chemical evolution models, should be a factor 3-4 bigger than the estimated by Pagel and Patchett (1975), which means $\simeq 10 \%$. In the definition of this quantity we have defined (halo)-thick-disk stars all those with $[\text{Fe}/\text{H}] < -1.0$ and thin disk stars all the others. However, these definitions should be taken with care in view of the fact that part of the low metallicity stars could have been accreted from satellites galaxies (Gratton et al. 1996), and therefore would not appear in our predictions. Our best model (model A) predicts a fraction of low metallicity stars in the range 6 – 10%, the exact value depending on the assumed duration of the thick disk phase (1 to 2 Gyrs). Model C, which assumes a timescale for the thick disk formation of 0.1 Gyrs, predicts a very high value for this fraction because in this case the thick disk evolution is faster, and more stars are formed during this phase. Models B and D predict very similar ratios which are smaller than in model A. In fact, the timescale for thin disk formation in models B and D is smaller than in model A and therefore they predict more thin disk stars and consequently a smaller ratio between metal poor stars and thin disk stars.

4.2. Supernova rates

The present SN rates in the Galactic disk were estimated by Van den Bergh (1988) as $0.6 h^2 \text{ century}^{-1}$ for type Ia SNe, $0.8 h^2 \text{ century}^{-1}$ for type Ib SNe and $2.2 h^2 \text{ century}^{-1}$ for type II SNe, assuming a total Galactic blue luminosity of $\simeq 2.0 \cdot 10^{10} L_{B\odot}$. In table 2 we are showing the values for $H = 50$ and $100 \text{ km s}^{-1} \text{ Mpc}^{-1}$ respectively, where an average value was taken for the type I SNe (Ia + Ib). Table 2 also shows the ratio between type II and type I SN rates. We can observe that our best model is in very good agreement with these constraints. For the other cases the predicted ratio is lower than the observed one. This is due, basically, to the lower rate of type II SNe predicted in models B, C and D. In fact, model A has a longer timescale for the formation of the thin disk relative to models B, C and D and, at present, is accreting more gas thus implying a higher star formation rate and type II SN rate (Table 2). This can be seen from the comparison of figures 4 and 6. This later shows the time evolution of type Ia and II supernovae. The temporal behaviour of type I SNe is almost independent of the details of the star formation rate as these objects have longer evolutionary timescales (see section 4.7).

4.3. The star formation history

As already mentioned in section 5, we adopt a threshold in the star formation rate which is responsible for the behaviour showed in figure 4. According to this threshold, the star formation stops when a surface gas density of $7 M_{\odot} \text{ pc}^{-2}$ is reached. This means that star formation can have an intermittent behaviour regulated by the surface gas density. In fact, after the threshold is reached and star formation stops the dying stars continue to restore gas into the interstellar medium and therefore, soon or later, the surface gas density will be again above the threshold and star formation will restart.

4.4. Present-Day Gas fraction

Our predicted value for the present-day gas fraction (Tosi 1996) is in agreement with the observational one for all the models of table 1. For the best model, however, the predicted present-day gas fraction is a little higher because of the slower evolution of the thin disk as implied by a timescale of mass accretion of 8 Gyrs.

4.5. Solar abundances

The solar abundances (by mass) predicted by the best model are compared with the observed ones (Anders and Grevesse 1989 - AG89) in table 3. These solar abundances are very similar in all the models shown in table 1. As already mentioned in section 2, these abundances should represent the composition of the interstellar medium at the time of the formation of the sun, e.g., 4.5 Gyrs ago. Since we assume a Galactic lifetime of 15 Gyrs this time corresponds to 10.5 Gyrs after the Big Bang. Given the uncertainties involved in observed determinations we can consider that the model is in agreement with the observed value inside a factor 2 difference. From table 3 we can see that only for two elements, namely 3He and Mg the model predictions fail. In the case of 3He this was expected as it constitutes a problem for almost all the chemical evolution models (Tosi 1996, Dearborn et al. 1995). For the Mg this can be attributed to the lower yield predicted for this elements by Woosley and Weaver (1995).

4.6. Age-Metallicity Relation

In figures 1a and 1b we present the age-metallicity relation for our best model compared, respectively, with two sets of observational data. From figure 1a, which presents

the data of Twarog (1980), Meusinger et al. (1991) and Carlberg et al. (1985), one can conclude that the model predictions agree quite well with the observational data. However, from the second set of data (Edvardsson et al. 1993), although there is an overall trend of decreasing mean metallicity with increasing age, a large scatter is present and we consider of fitting only the mean relation. According to Nissen (1995), however, the data of Edvardsson et al. should not be used to determine the mean age-metallicity relation in the solar neighbourhood as the sample of stars is biased with respect to $[\text{Fe}/\text{H}]$, in the sense that some metal rich stars have been excluded by a temperature cutoff. The same cutoff seems also to be present in Twarog’s data. Given this situation we cannot consider this constraint as a very tight one.

4.7. Stellar Metallicity Distributions

A very good agreement is obtained between the predictions of model A and the new data for the metallicity distribution of disk stars in the solar vicinity (figure 7). In this figure the observed metallicity distribution includes the thin disk stars as well as part of the thick disk ones, since the halo stars and the metal weak tail of the thick disk were excluded from the data by using a chemical criterion (all stars with $[\text{Fe}/\text{H}] < -1.2$). The same criterion has been used in the model predictions. The data have been corrected by the factor f , as defined by Sommer-Larsen (1991) in order to take into account the vertical scale height effects.

We stress that the comparison between model predictions and metallicity distribution is meaningful only when one considers explicitly the evolution of iron. Indeed, this can be done only by those models which take into account the type Ia SNe contribution. The majority of chemical evolution models consider IRA and does not take into account the type Ia SNe contribution to the chemical enrichment of the Galaxy. Thus, when comparing

theoretical predictions with observed chemical properties of our Galaxy, they are forced to use oxygen rather than iron. The solution often adopted in previous papers was to convert the observed $[\text{Fe}/\text{H}]$ into $[\text{O}/\text{H}]$ using a fit to the $[\text{O}/\text{Fe}]$ versus $[\text{Fe}/\text{H}]$ relation for solar vicinity stars, in order to do this conversion. Such a procedure is quite uncertain and if adopted in the framework of the present model produces quite different results from those obtained just comparing the real data ($[\text{Fe}/\text{H}]$) with the predicted $[\text{Fe}/\text{H}]$.

The metallicity distribution of metal poor stars constitutes another constraint. This metallicity distribution varies from author to author according the adopted selection criteria. According to Beers and Sommer-Larsen (1995) it is unlikely that these distributions are not a mixture of halo and thick disk populations whatever the criteria used, since the properties of both components overlap one another.

However, we are interested not to produce a fit of the metallicity distribution of metal poor stars but only to confirm that our models can predict a reasonable number of stars within a range in metallicity similar to the observed one. This was the case of model A, which predicts a reasonable number of stars with metallicities in the range $-3 \leq [\text{Fe}/\text{H}] \leq -1$. As an example model C which has τ_T equals to 0.1 Gyr predicts very few stars with metallicities $[\text{Fe}/\text{H}] < -2$ in contradiction with observations (Ryan and Norris 1991, Schuster et al. 1993, Laird 1995, Beers and Sommer-Larsen 1995).

Our best model (model A), which fits the disk metallicity distribution and predicts a number of stars which is in agreement with the metallicity distribution of metal poor stars, has a star formation in the thick disk more efficient than that in the thin disk ($\nu_T = 2.0$ and $\nu_D = 1.0 \text{Gyr}^{-1}$). However the exponent for the star formation rate is the same for the two phases ($k_T = k_D = 1.5$). We also ran models which have a higher star formation exponent in the thick disk compared to that in the thin disk and the same efficiency for the SFR, but they did not produce a good fit to the oxygen/iron relation. It should be noted, however,

that these parameter values must also be in agreement with all the other constraints for the chemical evolution models. For instance, a very high SFR in the thick disk would produce a lot of metal-poor stars leading to a too high ratio of low-metallicity/thin-disk stars.

Model A predicts a timescale for the thick and thin disk formation of, respectively, ≤ 1 Gyr and 8 Gyr. Timescales of this order have been suggested also by the results of chemo-dynamical models of Burkert et al. (1992) and recently by Yoshii et al. (1996). The τ_T value cannot be much less than 1 Gyr because in such a case the model would predict a metallicity distribution for metal-poor stars which is shifted towards a metallicity higher than the observed one, as a consequence of the faster evolution of the thick disk (model C). On the other hand, a value greater than 1 Gyr, would produce a model which does not agree with the observed behaviour of the oxygen to iron ratio (i.e. the long plateau in [O/Fe]) and which also predicts too many metal poor stars in the disk (G-dwarf problem). Concerning the timescale for the (halo)-thick-disk formation, the high value for τ_D is necessary to fit the new observed G-dwarf distribution for disk stars which shows a much more pronounced peak for intermediate metallicities than the previous one. Models with $\tau_D \leq 6$ Gyr lead to a poor agreement with the metallicity distribution by Rocha-Pinto and Maciel (1995). This explains the larger timescale obtained by the present model compared with that found by MF89, which was 3-4 Gyrs, and also the higher exponent k of the star formation rate.

4.8. The [O/Fe] versus [Fe/H] relation

The distribution of the abundance ratios represents an important constraint for chemical evolution models. In fact, they are less dependent on model parameters than absolute abundances, since depend essentially on the nucleosynthesis yields. Figure 3 shows the oxygen/iron ratio with respect to iron relative to the sun. Our best model (Model A) is represented by the solid line in this figure. Although our models predict an overabundance

of oxygen for the halo stars, the predicted $[O/Fe]$ is lower than the observed mean value. This is a consequence of the high iron yield for type II SNe taken from Woosley and Weaver (1995). This fact indicates that the iron yields from type II SNe should be lower, as also discussed by Timmes et al. (1995).

Figure 8 shows the star formation rate for a model (model C) with a timescale for the thick disk shorter than in model A. It can be seen that in models with a short thick disk timescale the gap in the star formation which arises between the thick and thin disk phases lasts longer (compare figure 4 and figure 8). This is a consequence of the faster consumption of gas together with the threshold in the star formation rate, and in a such case the model predicts a looping in the oxygen to iron ratio as function of metallicity (dotted line in figure 2). The looping predicted by the two infall model, also suggested by observations (see Gratton et al. 1996 and references therein), can be understood as to be caused by the strong dilution of the interstellar medium abundances at the moment of maximum infall onto the disk coupled to a sudden decrease of the SFR at the end of the halo-thick disk phase. The dilution lowers the absolute abundances but does not affect their ratios, whereas a gap in the SFR would lower the oxygen abundance (whose progenitors are mainly the type II SNe), but not that of iron which continues to grow due to the contribution of the type Ia SNe. However, the star formation gap lasts for a very short time because of the gas which is setting onto the disk at a high rate, and so the decrease in the $[O/Fe]$ ratio is much smaller than the decrease in the iron abundance, as can be observed in figure 3. However, since we need relatively long timescale (1 Gyr) for the halo and thick disk formation our best model does not present a very pronounced star formation gap (see fig. 4). The net effect on the $[O/Fe]$ versus $[Fe/H]$ relationship is that the oxygen overabundance (as well for the other elements) does not remain constant until the disk formation ($[Fe/H] \simeq -1$), but starts to decrease slowly from lower metallicities. This can be understood as a non negligible contribution of type Ia SNe already in the thick disk phase.

We have also computed models with delayed infall but without the star formation threshold and with an artificially imposed gap on the SFR at the end of the thick disk phase. In this case we have seen that the star formation in the thick disk should be almost of the same order as that in the thin disk, in order to avoid an overproduction of both oxygen and iron by the type II SNe in the thick disk phase, resulting in a solar ratio in poor agreement with observations, which, in turn, gives extremely high $[O/Fe]$ ratios for $[Fe/H] < -1$. A better agreement between observational constraints and theoretical predictions is achieved when the SFR in the (halo)-thick-disk is more efficient than that of thin disk, as also suggested by Larson (1976).

4.9. The $[X/Fe]$ versus $[Fe/H]$ relation for the other elements studied

Figures 9 a,b,c,d show the predicted abundances of α -elements (Mg, Si, S and Ca) relative to iron as functions of $[Fe/H]$ compared with observational data. Generally, although the spread in the data is due mainly to the fact that the data originate from different sources, the agreement is acceptable. There is, as already mentioned, a general problem with the iron yields from supernovae of type II which is probably too high. However, the agreement between predictions and observations is generally quite satisfactory, perhaps with the exception of S.

In figure 10 (a, b) the model predictions for Zn and Cu are compared with the observations. For Zn and Cu there is a marginal agreement, with the curves which lie below the observational data. This is also a consequence of the high iron yield predicted by the Woosley and Weaver (1995) stellar evolution models. An extended discussion about these elements is present by Matteucci et al. (1993).

Figure 11 shows the $[C/Fe]$ versus $[Fe/H]$ relation. For this element, which is mostly

produced by low- and intermediate-mass stars, as iron, we should expect a constant and solar ratio. As in the MF89 model, the predicted $[C/Fe]$ ratio shows a small bump around $[Fe/H] = -1.0$, which should be due to the assumption of not fully consistent nucleosynthesis yields in the ranges of massive and low- and intermediate- mass stars. On the other hand, the observational data for this element show a considerable scatter. Our predictions for C seem also to predict a positive trend for metallicities smaller than about $[Fe/H] \simeq -2$.

Figure 12 shows the behaviour of nitrogen. For this element the data also seem to indicate a big scatter. Moreover, as discussed in Timmes et al. (1995), in the data of Laird (1985) there is a zero-point correction factor of $\sim +0.65$ dex. All of this makes the situation for nitrogen quite uncertain and more and better data are required. Our predictions show an initial steep increase of the $[N/Fe]$ ratio due to the fact that the first N which is produced originates from massive stars as a secondary element. Moreover, the nitrogen produced in intermediate and low mass stars is also mostly secondary, although some primary N can be produced in massive intermediate mass stars (Renzini and Voli, 1981), but the exact amount is quite uncertain. A higher $[N/Fe]$ ratio at low $[Fe/H]$ could be obtained only by assuming that N in massive stars has a primary origin (Matteucci 1986; Timmes et al. 1995). Primary N in massive stars seems to be required also to explain the abundance pattern in damped Ly- α systems (Matteucci et al. 1996).

Figure 13 shows the predictions for the $\log(X/O)$ versus O/H relationship for S, N, C and Ne. The Ne/O and S/O ratios as function of oxygen are almost constant, an expected fact since these elements are produced in the same stars as oxygen. The growth of the N/O ratio is showing again the assumed secondary origin of nitrogen in massive stars. The increase of the C/O ratio with oxygen is due to the fact that carbon is mostly produced in low- and intermediate-mass stars whereas most of the oxygen comes from the massive star

range.

4.10. Radial Profiles

Here we discuss the predicted radial properties of our best model A.

Figure 14 shows the predicted $[\text{O}/\text{Fe}]$ versus $[\text{Fe}/\text{H}]$ relations for three different galactocentric distances (4, 10 and 14 kpc). As first pointed out by Matteucci (1992), the slope of the $[\text{O}/\text{Fe}]$ in the thin disk metallicity range steepens with increasing galactocentric distance as due to the differential evolution of the thin disk. Here, another effect of this differential evolution appears, namely a loop in the $[\text{O}/\text{Fe}]$ develops at 4 kpc. This is due to the higher maximum infall at this galactocentric distance relative to larger distances.

As shown by Rana (1991), the distribution of neutral and molecular hydrogen in the Galaxy is poorly known and independent observations do not agree with each other. In figure 15 we compare our model predictions for the radial gas distribution with the observed one (taken from Rana 1991, table 3). Given the uncertainties in the observational data, we can say that the model is in agreement with the observed radial profile. Some disagreement, however, seems to arise for galactocentric distances smaller than 4 kpc, where the model predicts much more gas than is observed. A possible solution to this problem could be the existence of a bar in our Galaxy which would strip the gas and push it into the Galactic center. For the outer radii the model predicts a flat distribution but observational data are not available.

The observed radial dependence of the present time star formation rate is also very uncertain. Usually pulsars, supernovae remnants and Ly continuum photons are used as tracers of the present star formation rate across the disk. However, as discussed by Kennicutt (1989) for the purpose of chemical evolution model calculations, a global star

formation rate process should be taken into account instead of local ones. So it is not clear if this comparison is meaningful given the large uncertainties involved. One example of this kind of problem is the apparent lack of correlation, found by Kennicutt, between the radial distribution of the global star formation rate and molecular clouds in external galaxies.

Table 4 shows the gradients predicted by our best model for the inner ($4 \leq R(kpc) \leq 10$) and outer ($10 \leq R(kpc)$) regions of the Galactic disk as functions of time, for O, Fe, N, S and Ne. The same is shown for D, 3He and 4He in table 5. The quoted errors represents the confidence of the theoretical bestfits. The gradients are shown also as functions of Galactic ages, namely 15, 12, 10.5 (t_{\odot}), 7 and 2 ($t_{infallmax}$) Gyrs. Our best model predicts a steeper gradient in the inner regions, which grows with time and a flatter one in the outer parts. As discussed in section I, this result seems to be in agreement with the observational data. We note that one of the consequences in adopting a differential formation of the thin disk is that we expect different time histories of gradients in the inner and outer regions. In particular, the gradients in the outer regions grow quicker than those in the inner regions but reach very soon a saturation value. This is due to the fact that in the outer regions the threshold value in the gas density is reached very early, due to the lower gas density always present there, whereas in the inner regions such as 4 kpc the threshold is not yet reached at the present time.

5. Discussion and Conclusions

In this paper we presented a model for the chemical evolution of the Galaxy assuming that the formation of thick disk and thin disk occurred in two main accretion episodes. New stellar yields and a threshold in the star formation process were also considered. From the comparison between observational constraints and our theoretical results, we can conclude that the two-infall model is in good agreement with most of the observed features of the

Galaxy. Our main conclusions are:

- Our best model predicts the abundances of 16 chemical elements well in agreement with the observed solar abundances with the exception of ${}^3\text{He}$ and Mg. The behaviours of relative ratios as functions of $[\text{Fe}/\text{H}]$ also agree with the available observational data although the comparison between theory and observations suggest to lower the iron yield from type II SNe and to increase the Mg yield from type II SNe. The same conclusion concerning Fe was reached by Timmes et al. (1995) who adopted the same yields.
- The assumption of a threshold for the star formation naturally leads to a star formation gap at the end of the halo and thick disk phases as suggested by Gratton et al. (1996), and prevents an overproduction of oxygen by halo stars. This star formation gap reflects in a more or less pronounced decrease in the $[\alpha/\text{Fe}]$ ratios around $[\text{Fe}/\text{H}] = -0.6$ dex, depending on the duration of the gap itself.
- The $[\alpha/\text{Fe}]$ versus $[\text{Fe}/\text{H}]$ relations for stars born at different radii than the solar circle indicate that a loop in the $[\alpha/\text{Fe}]$ develops at small galactocentric distances.
- Our best model predicts a stellar metallicity distribution for the G-dwarfs in the disk in very good agreement with the new observations (Rocha-Pinto and Maciel 1996, Wyse and Gilmore 1995). This constitutes the most important constraint for chemical evolution models at present and implies a timescale for disk formation much longer than that for the formation of the halo (and thick disk).

A reasonable agreement is found also when comparing the predicted and observed number of very low metallicity stars (Ryan and Norris 1991, Schuster et al. 1993, Laird 1995, Beers and Sommer-Larsen 1995). The model predicts a timescale of 1 Gyr for the formation of the halo and thick disk and 8 Gyr for the formation of the thin

disk in the solar vicinity.

The agreement with the metallicity stellar distribution and also with the fraction of metal poor stars, in the solar neighbourhood, constitutes an important and new result being a consequence of, at least, three main assumptions of our model. First, the decoupling between the rate of gas loss from the halo-thick disk and that of gas infalling onto the thin disk, allowing a much longer timescale for the thin disk evolution as compared to that of the thick disk phase. Second, the delay in the beginning of the thin disk evolution, which characterizes a sequential model, at variance with the models of Matteucci et al (1990), Pardi and Ferrini (1994) and Pardi et al. (1995) which adopt the view of a parallel evolution of all galactic components (halo, thick and thin disk) at different evolutionary rates. These models which consider a superposition of stellar populations, evolving simultaneously do not best fit the distinct enrichment histories of the different components at the same time. Finally, the third reason, is a threshold in the star formation rate which limits the star formation in the halo phase allowing for the formation of a number of stars with small metallicities as required by the metallicity distribution of metal poor stars.

- Our best model requires a more steep dependence of the surface gas density ($k = 1.5$) compared to what was previously reported by MF89 ($k = 1.1$). It has also been shown that the star formation exponent should be the same for thick and thin disk phases in order to reproduce the observational constraints. However, during the thick disk phase the star formation should be more efficient and this is obtained by adopting a bigger value for the efficiency of star formation, the constant $\tilde{\nu}_T$. Dopita and Ryder (1994) have investigated various models of star formation in disk galaxies. These authors showed that the star formation rate in disk galaxies determines their stellar surface brightness and the surface brightness in $H\alpha$. From a star formation rate of the same type of the one used here, but expressed in a more general form

($\Psi \propto \sigma_g^m \sigma_T^n$), they claim that a satisfactory agreement with the observed properties of such galaxies is achieved for $1.5 < m + n < 2.5$. In terms of our formulation, this means: $1.25 < k < 1.75$, which is in extremely good agreement with our best model prediction of $k = 1.5$. Prantzos and Aubert (1995) investigated the effect of different assumptions about the star formation rate on chemical evolution models. They tested also the one given by Dopita and Ryder (1994), for the cases $n = 1, m = 1$ and $n = 0.5, m = 1$ and concluded, at variance with us, that a star formation rate given by the expression above, which depends not only on the gas mass density but also on the total mass density, did not fit all the required constraints, and adopted instead a star formation rate given by: $\Psi \propto (1/R) \sigma_g(R)^n$ which reproduces the steep distribution of the star formation rate given by the observational data. The authors argued that the discrepancy between the SFR proposed by Dopita and Ryder (1994) and the observational constraints was due to a too steep radial dependence leading to an overestimation of the amount of gas in the outer parts of the Galaxy. However, given our results, we suggest that Prantzos and Aubert (1995) did not find an agreement between the star formation proposed by Dopita and Ryder (1994) and the observational properties because of the mild dependence on the gas mass density they adopted.

- Steeper abundance gradients for O, N and S are predicted for the inner regions of the Galactic disk ($R < R_\odot$) relative to the outer regions. This result is in agreement with recent abundance determination in B supergiants (Kaufer et al. 1994) and with abundance measurements of HII regions (Vilchez and Esteban 1996; Simpson et al. 1995). The gradients obtained by MF89 were generally steeper than the present ones although the difference between the inner and outer regions was already present. The difference between the present results and those of MF89 is to ascribe mainly to the adoption of a threshold in the gas density which regulates the process

of star formation, preventing the growth of abundances in the outer regions due to the constantly low amount of gas. We have computed also the evolution of such gradients in time and found that the inner gradients generally steepen in time. This is a consequence of the slow formation of the Galactic disk.

Finally, we would like to discuss briefly the roles of the different free parameters. The model presented here has essentially four free parameters namely k , ν , τ_T and τ_D . The parameters ν and k of the star formation rate both influence the absolute abundances and k influences also the shape of the distribution of the gas along the disk. After performing several numerical experiments, we found the range of permitted values for k is 1.5 ± 0.2 . The parameter τ_T is constrained to be 1 ± 0.3 Gyr by the $[\alpha/\text{Fe}]$ plateau and the parameter τ_D is constrained by the G-dwarf metallicity distribution. We found that the range of acceptable values for τ_D in the solar neighbourhood to be 8 ± 1.5 Gyrs.

Our model can be further improved if we take into account the following points:

- Preliminary results for the radial profiles have shown that the SFR and gas radial distributions along the disk of the Galaxy are flat in the outer parts. This behavior is clearly a consequence of the star formation threshold. Note, however, that a flat gas distribution is observed for HI whereas that of H_2 decreases with the galactocentric distance. As a consequence, we should consider models with these two gas phases separately (the subject of a future paper).
- The predicted solar and present 3He abundance is very high in comparison with the observed values. This occurs for a large fraction of the presently available chemical evolution models (Tosi 1996). In our models the 3He abundance grows rapidly after the time of the formation of the sun. This is due to the fact that this is exactly

the moment when the stars with masses smaller than $1.4M_{\odot}$, which are the main producers of ${}^3\text{He}$, die.

- The predicted helium-to-metals enrichment ratio is 1.6 which is much smaller than the observed one which lies between 4 and 5 (Chiappini and Maciel 1994, Pagel et al. 1992). However, the observed value is based on gaseous nebulae abundances which could be uncertain. On the other hand, the predicted value for this ratio is very dependent on the adopted nucleosynthesis prescriptions. There are many possibilities which could be considered: a revised ${}^4\text{He}$ or heavy element nucleosynthesis, or the formation of black holes instead of SN explosions in massive stars above a certain mass.
- We should find a more physically justified parameterization for radial variation of the infall timescale in the disk.
- We should also investigate the dust influence on chemical evolution models (also a subject for a future paper)

acknowledgments - C. C. and F. M. want to thank the SISSA institute and the Department of Astronomy of the University of Trieste for their kind hospitality. We also thank the referee Jesper Sommer-Larsen for his useful suggestions. This work was partially supported by CNPq/Brazil

Table 1: Input Parameters for the solar neighbourhood

Model	$\tilde{\nu}_T$ (Gyr^{-1})	k_T	$\tilde{\nu}_D$ (Gyr^{-1})	k_D	τ_T (Gyr)	τ_D (Gyr)
A	2.0	1.5	1.0	1.5	1.0	8.0
B	2.0	1.5	1.0	1.5	1.0	5.0
C	2.0	1.5	1.0	1.5	0.1	5.0
D	2.7	2.0	1.0	1.5	1.0	5.0

Table 2: Current predicted and observed quantities for the solar neighbourhood

	A	B	C	D	Observations
metal-poor/total stars	6-13 %	5-10 %	17 %	5-10 %	$\simeq 10$ %
$\text{SNI } \textit{century}^{-1}$	0.29	0.37	0.37	0.38	0.17-0.7
$\text{SNII} \textit{century}^{-1}$	0.78	0.53	0.54	0.55	0.55-2.2
SNII/SNI	2.7	1.4	1.5	1.4	3.1
$\Psi(R_{\odot}, t_{\text{now}})$ $M_{\odot} \textit{pc}^{-2} \textit{Gyr}^{-1}$	2.64	2.38	2.34	2.38	2-10
$\sigma_g(R_{\odot}, t_{\text{now}})$ $M_{\odot} \textit{pc}^{-2}$	7.0	7.0	7.0	7.0	6.6 ± 2.5
$\sigma_g/\sigma_T(R_{\odot}, t_{\text{now}})$	0.14	0.12	0.11	0.12	0.05-0.20
$\sigma_{\text{inf}}(R_{\odot}, t_{\text{now}})$ $M_{\odot} \textit{pc}^{-2} \textit{Gyr}^{-1}$	1.05	0.73	0.73	0.73	1.0
$\Delta Y/\Delta Z$	1.63	1.60	1.57	1.60	3.5 ± 0.7
$\Psi(R_{\odot}, t_{\text{now}})/\langle \Psi \rangle$	~ 0.7	~ 0.7	~ 0.7	~ 0.7	0.18-3.0

Table 3: Solar Abundances by Mass

Element	Best Model (A)	Observations (AG89)
<i>H</i>	.731	.702
<i>D</i>	4.630 (-5)	4.80 (-5)
³ <i>He</i>	10.01 (-5)	2.93 (-5)
⁴ <i>He</i>	2.548 (-1)	2.75 (-1)
¹² <i>C</i>	1.827 (-3)	3.03 (-3)
¹⁶ <i>O</i>	7.278 (-3)	9.59 (-3)
¹⁴ <i>N</i>	1.386 (-3)	1.11 (-3)
¹³ <i>C</i>	4.758 (-5)	3.65 (-5)
<i>Ne</i>	0.942 (-3)	1.62 (-3)
<i>Mg</i>	2.48 (-4)	5.15 (-4)
<i>Si</i>	7.03 (-4)	7.11 (-4)
<i>S</i>	3.071 (-4)	4.18 (-4)
<i>Ca</i>	3.95 (-5)	6.20 (-5)
<i>Fe</i>	1.37 (-3)	1.27 (-3)
<i>Cu</i>	8.18 (-7)	8.40 (-7)
<i>Zn</i>	2.44 (-6)	2.09 (-6)
<i>Z</i>	1.433 (-2)	1.886 (-2)

Table 4: Abundance gradients (dex/kpc)

Time (Gyr)	inner region	outer region
O		
15	-0.032 ± 0.005	-0.018 ± 0.001
12	-0.023 ± 0.006	-0.017 ± 0.001
10.5	-0.018 ± 0.007	-0.017 ± 0.001
7	-0.003 ± 0.005	-0.014 ± 0.001
2	0	0
Fe		
15	-0.040 ± 0.008	-0.017 ± 0.002
12	-0.027 ± 0.010	-0.014 ± 0.002
10.5	-0.020 ± 0.009	-0.013 ± 0.001
7	-0.001 ± 0.007	-0.010 ± 0.001
2	0	0
N		
15	-0.037 ± 0.005	-0.028 ± 0.002
12	-0.027 ± 0.007	-0.027 ± 0.002
10.5	-0.021 ± 0.008	-0.026 ± 0.003
7	-0.002 ± 0.007	-0.022 ± 0.002
2	0	0
S		
15	-0.036 ± 0.006	-0.021 ± 0.001
12	-0.025 ± 0.008	-0.019 ± 0.001
10.5	-0.019 ± 0.008	-0.019 ± 0.001
7	-0.003 ± 0.006	-0.015 ± 0.001
2	0 ± 0	0 ± 0
Ne		
15	-0.030 ± 0.004	-0.019 ± 0.001
12	-0.023 ± 0.006	-0.020 ± 0.001
10.5	-0.018 ± 0.006	-0.021 ± 0.001
7	-0.004 ± 0.005	-0.018 ± 0.001
2	0 ± 0	0 ± 0

Table 5: Abundance gradients (dex/kpc)

Time (Gyr)	inner region	outer region
D		
15	0.026 ± 0.008	0.003 ± 0.001
12	0.009 ± 0.004	0.002 ± 0
10.5	0.005 ± 0.003	0.001 ± 0
7	0 ± 0	0.001 ± 0
2	0	0
${}^3\text{He}$		
15	-0.027 ± 0.018	-0.006 ± 0.002
12	-0.001 ± 0.015	0 ± 0
10.5	0.005 ± 0.011	0.003 ± 0.001
7	0.005 ± 0.004	0.004 ± 0.001
2 0	0	
${}^4\text{He}$		
15	-0.006 ± 0.001	-0.002 ± 0.000
12	-0.004 ± 0.001	-0.002 ± 0.000
10.5	-0.003 ± 0.001	-0.002 ± 0.000
7	0	-0.001
2	0	0

REFERENCES

- Anders, E., Grevesse, N. 1989, *Geochim. Cosmochim. Acta* 53, 197
- Beers, T. C., Sommer-Larsen, J. 1995, *ApJ. Supp.* 96, 175
- Burkert, A., Truran, J., Hensler, G. 1992, *ApJ* 391, 651
- Carigi, L. 1994, *ApJ* 424, 181
- Carbon, D. F., Barbu, B., Kraft, R. P., Friel, E. D. 1987, *PASP* 99, 335
- Carlberg, R. G., Dawson, P. C., Hsu, T., Vandenberg, D. A. 1985, *ApJ* 294, 674
- Chiappini, C., Maciel, W. J. 1994 *A & A* 288, 921
- Chiosi, C. 1980, *A & A* 83, 206
- Clegg, R. E. S., Lambert, D. L., Tomkin, J. 1981, *ApJ* 250, 262
- Cunha, K., Lambert, D. 1992, in *Origin and Evolution of the Elements*, eds. N. Prantzos, E. Vangioni-Flam and M. Cassé, Cambridge Univ. Press, p. 274
- Dearborn, D. S. P., Steigman, G., Tosi, M. 1995, *ApJ* (submitted)
- Dopita, M. A. 1985, *ApJ* 295, L5
- Dopita, M. A., Ryder, S. D. 1994, *ApJ* 430, 163
- Edvardsson, B., Andersen, J., Gustafsson, B., Lambert, D. L., Nissen, P. E., Tomkin, J. 1993, *A & A* 275, 101
- Ferrini, F., Mollá, M., Pardi, M. C., Díaz, A. I. 1994, *ApJ.* 427, 745
- François, P. 1986, *A & A* 160, 264

- François, P. 1987, A & A 176, 294
- François, P. 1988, A & A 195, 226
- François, P., Matteucci, F. 1993, A & A 280, 136
- Gibson, B., K. 1996, MNRAS (in press)
- Giovagnoli, A., Tosi, M. 1995, MNRAS 273, 499
- Gratton, R., Carretta, E., Matteucci, F., Sneden, C. 1996, A & A (submitted)
- Gratton, R. G., Ortolani, S. 1986, A& A 169, 201
- Gratton, R. G., Sneden, C. 1994, A & A 287, 927
- Gratton, R. G., Sneden, C. 1991, A & A 241, 501
- Gratton, R. G., Sneden, C. 1988, A & A 204, 193
- Gratton, R. G., Sneden, C. 1987, A & A 178, 179
- Greggio, L., Renzini, A. 1983, A & A 118, 217
- Ibata, R. A., Gilmore, G. 1995, MNRAS 275, 605
- Kaufer, A., Szeifert, Th., Krenzin, R., Basckek, B., Wolf, B. 1994, A & A 289, 740
- Kennicutt, R. C. 1989, ApJ 344, 685
- Kraft, R. P., Sneden, C., Langer, G. E., Prosser, C. F. 1992, AJ 104, 645
- Lacey, C. G., Fall, S. M. 1985, ApJ 290, 154
- Laird, J. B. 1995 (private com. - data from Carney, B. W., Lathan, D. W., Laird, J. B.,
Aguilar, L. A. 1994, AJ 107, 2240)

- Laird, J. B. 1985, ApJS 289, 556
- Larson, R. B. 1976, MNRAS 176, 31
- Liu, X. -W., Barlow, M. J., Danziger, I. J., Storey, P. J. 1995 (in preparation)
- Maciel, W. J., Chiappini, C. 1994, Astrophys. Sp. Sci. 219, 231
- Maciel, W. J., Köppen, J. 1994, A & A 282, 436
- Magain, P. 1989, A & A 209, 211
- Magain, P. 1987, A & A 179, 176
- Malinie, G., Hartmann, D. H., Clayton, D. D., Mathews, G. J. 1993, ApJ. 413, 633
- Marigo, P., Bressan, A., Chiosi, C. 1996 A & A (in press)
- Matteucci, F., 1994, IAU Symp. 169, The Hague (in press)
- Matteucci, F. 1986, PASP 98, 973
- Matteucci, F. 1992, in *Morphological and Physical Classification of Galaxies*, ed. G. Longo et al., Kluwer Academic Publ., p.245
- Matteucci, F., Brocato, E. 1990, ApJ 365, 539
- Matteucci, F., Ferrini, F., Pardi, C., Penco, U. 1990, in *Chemical and dynamical evolution of galaxies*, eds. F. Ferrini, J. Franco and F. Matteucci, ETS Editrice, PISA, p.586
- Matteucci, F., François, P. 1989, MNRAS 239, 885
- Matteucci, F., François, P. 1992, A & A 262, L1
- Matteucci, F., Greggio, L. 1986, A & A 154, 279

- Matteucci, F., Raiteri, C. M., Busso, M., Gallino, R., Gratton, R. G. 1993, A& A 272, 421
- Matteucci, F., Molaro, P., Vladilo, G. 1996, A & A submitted
- Meusinger, H., Reimann, H. G., Stecklum, B. 1991, A & A 245, 57
- Nissen, P. E. 1995, in *Stellar Populations*, IAU Symp. 164, ed. P. C. van den Kruit and G. Gilmore, the Haghe, Kluwer, Dordrecht, p. 109
- Nissen, P. E., Edvardsson, B. 1992, A & A 261, 255
- Nomoto, K., Thielemann, F. K., Yokoi, K. 1984, ApJ 286, 644
- Pagal, B. E. J. 1989, in *Evolutionary Phenomena in Galaxies*, eds. J. E. Beckman and B. E. J. Pagal, Cambridge Univ. Press, p. 201
- Pagal, B. E. J., Patchett, B. E. 1975, MNRAS 172, 13
- Pagal, B. E. J., Simonson, E. A., Terlevich, R. J., Edmunds, M. G. 1992, MNRAS 255, 325
- Pagal, B. E. J., Tautvaisiene, G. 1995, MNRAS 276, 505
- Pardi, C., Ferrini, F. 1994, ApJ 421. 491
- Pardi, C., Ferrini, F., Matteucci, F. 1995, ApJ 444, 207
- Prantzos, N., Aubert, O. 1995, A & A 302, 69
- Rana, N. 1991, ARA& A 29, 129
- Rocha-Pinto, H. J., Maciel, W. J. 1996, MNRAS 279, 447
- Renzini, A., Voli, M. 1981, A & A 94, 175
- Ryan, S.G., Norris, J. E. 1991, AJ 101, 1865

- Samland, M., Hensler, G. 1996, Review in Modern Astronomy 9 (in press)
- Scalo, J. M. 1986, Fund. Cosmic Phys. 11, 1
- Schuster, W. J., Parrao, L., Contreras Martinez, M. E. 1993, A & A Supp. 97, 951
- Shaver, P. A., McGee, R. X., Newton, L. M., Danks, A.C., Pottasch, S. R. 1983, MNRAS 204, 53
- Simpson, J.P., Colgan, S.W.J., Rubin, R.H., Erickson, E.F., Haas, M.R. 1995, ApJ 444, 721
- Snedden, C., Crocker, D. A. 1988, ApJ 335, 406
- Snedden, C., Kraft, R. P., Prosser, C. F., Langer, G. E. 1991, AJ 102, 2001
- Snedden, C., Gratton, R. G., Crocker, D. A. 1991b, A & A 246, 354
- Sommer-Larsen, J. 1991, MNRAS 249, 368
- Sommer-Larsen, J., Yoshii, Y. 1990, MNRAS 243, 468
- Sommer-Larsen, J., Yoshii, Y. 1989, MNRAS 238, 133
- Talbot, R. J., Arnett, W. D. 1975, ApJ 197, 551
- Thielemann, F. K., Nomoto, K., Hashimoto, M. 1993, in *Origin and Evolution fo the Elements*, eds. N. Prantzos, E. Vangioni-Flam and M. Cassé, p. 297, Cambridge University Press
- Timmes, F. X., Woosley, S. E., Weaver, T. A. 1995, ApJS 98, 617
- Tomkin, J., Lemke, M., Lambert, D. L., Sneden, C. 1992, AJ 104, 1568
- Tomkin, J., Sneden, C., Lambert, D. L. 1986, ApJ 302, 415
- Tomkin, J., Lambert, D. L., Balachandran, S. 1985, ApJ 290, 289

- Tosi, M. 1996, in *From Stars to Galaxies*, PASP (in press)
- Tosi, M. 1988, *A & A* 197, 47
- Tsujiimoto T., Yoshii, Y., Nomoto, K., Shigeyama, T. 1995, *A & A* 302, 704
- Twarog, B. A. 1980, *ApJ* 242, 242
- van den Bergh, S. 1988, *Comments Astrophys.* XII, No.3, p. 131
- Vilchez, J. M., Esteban, C. 1996, *MNRAS* (in press)
- Woosley, S. E., Weaver, T. A. 1995, *ApJS* 101, 181
- Woosley, S. E., Weaver, T. A. 1986, *IAU Colloq.* 89, eds. D. Mihalas and K. H. Winkler,
Reidel, Dordrecht, p. 91
- Wyse, R. F. G., Gilmore, G. 1995, *AJ* 110, 2771
- Wyse, R. F. G., Gilmore, G. 1992, *AJ* 104, 144
- Yoshii, Y., Tsujimoto, T., Nomoto, K. 1996, *ApJ.* (in press)
- Zhao, G., Magain, P. 1990, *A & A* 238, 242

Figure Captions

Fig. 1 - Age metallicity relation for two different data sets. The curve shows the best model prediction

Fig. 2 - Observed G-dwarf metallicity distributions at the solar vicinity

Fig. 3 - [O/Fe] versus [Fe/H] behaviour for model A (solid line) and model C (dotted line)

Fig. 4 - Temporal evolution of the star formation rate as predicted by model A for the solar vicinity

Fig. 5 - Masses ejected in the form of various elements weighted by the IMF, are plotted as functions of the initial mass of the progenitor star

Fig. 6 - Temporal evolution of type Ia and type II SNe as predicted by model A for the solar vicinity

Fig. 7 - G-dwarf metallicity distribution in the solar vicinity predicted by model A. The data are from Rocha-Pinto and Maciel (1995)

Fig. 8 - Temporal evolution of the star formation rate, at solar vicinity, as predicted by model C

Fig. 9 - Predicted behaviour of the relative ratios of several heavy elements to iron with respect to the relative iron abundance, in the solar neighbourhood a) for Mg, b) for Si c) for S and d) for Ca

Fig. 10 - Same as figure 10 for a) Zn and b) Cu

Fig. 11 - Same as figure 10 for C

Fig. 12 - Same as figure 10 for N

Fig. 13 - $\log(X/H)$ versus O/H relation as predicted by model A

Fig. 14 - $[O/Fe]$ vs $[Fe/H]$ relations for three different galactocentric radii

Fig. 15 - Radial distribution of the present surface gas density. The data are from Rana (1991). Solid line represents model A prediction.

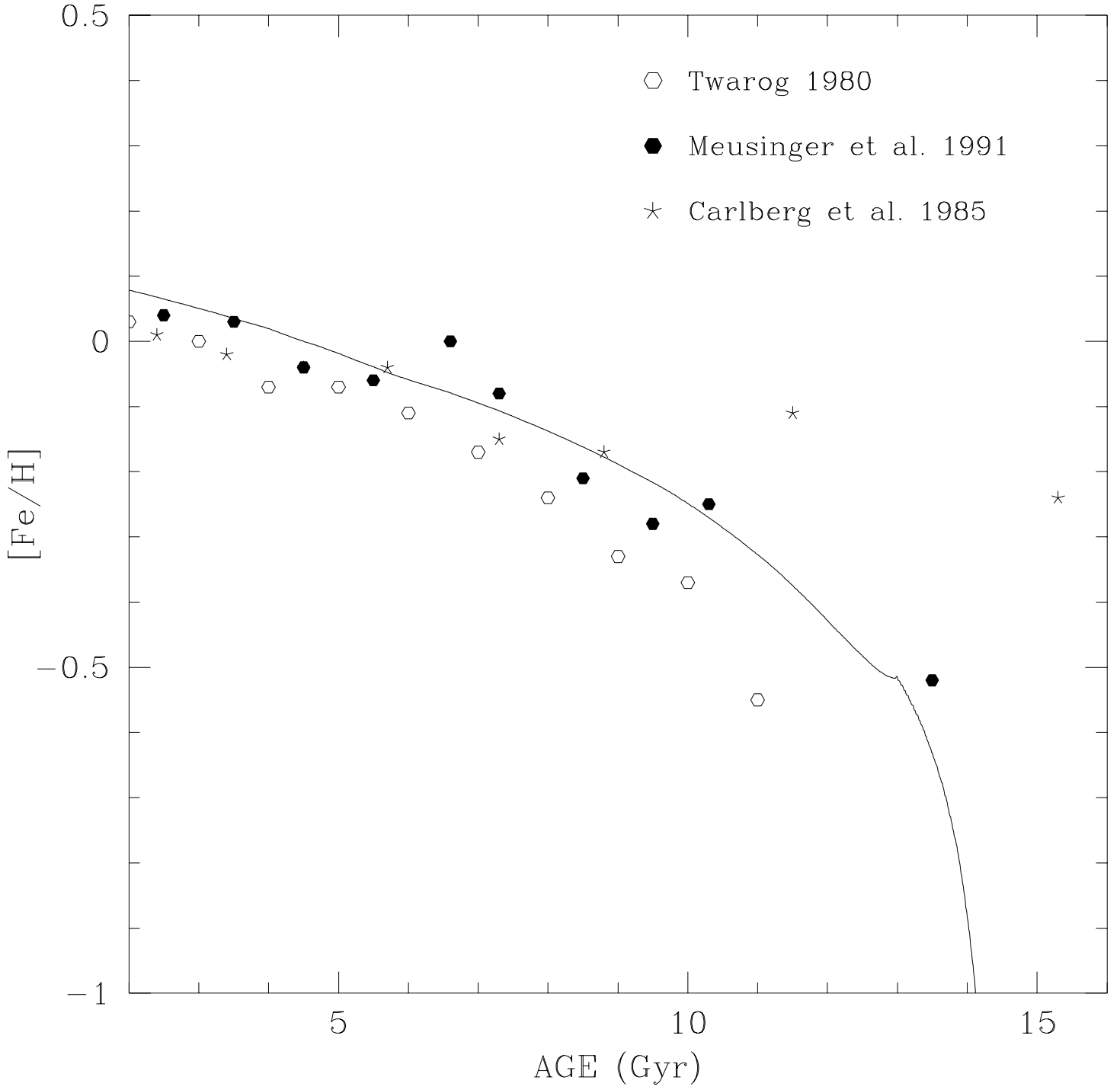


Fig. 1a.—

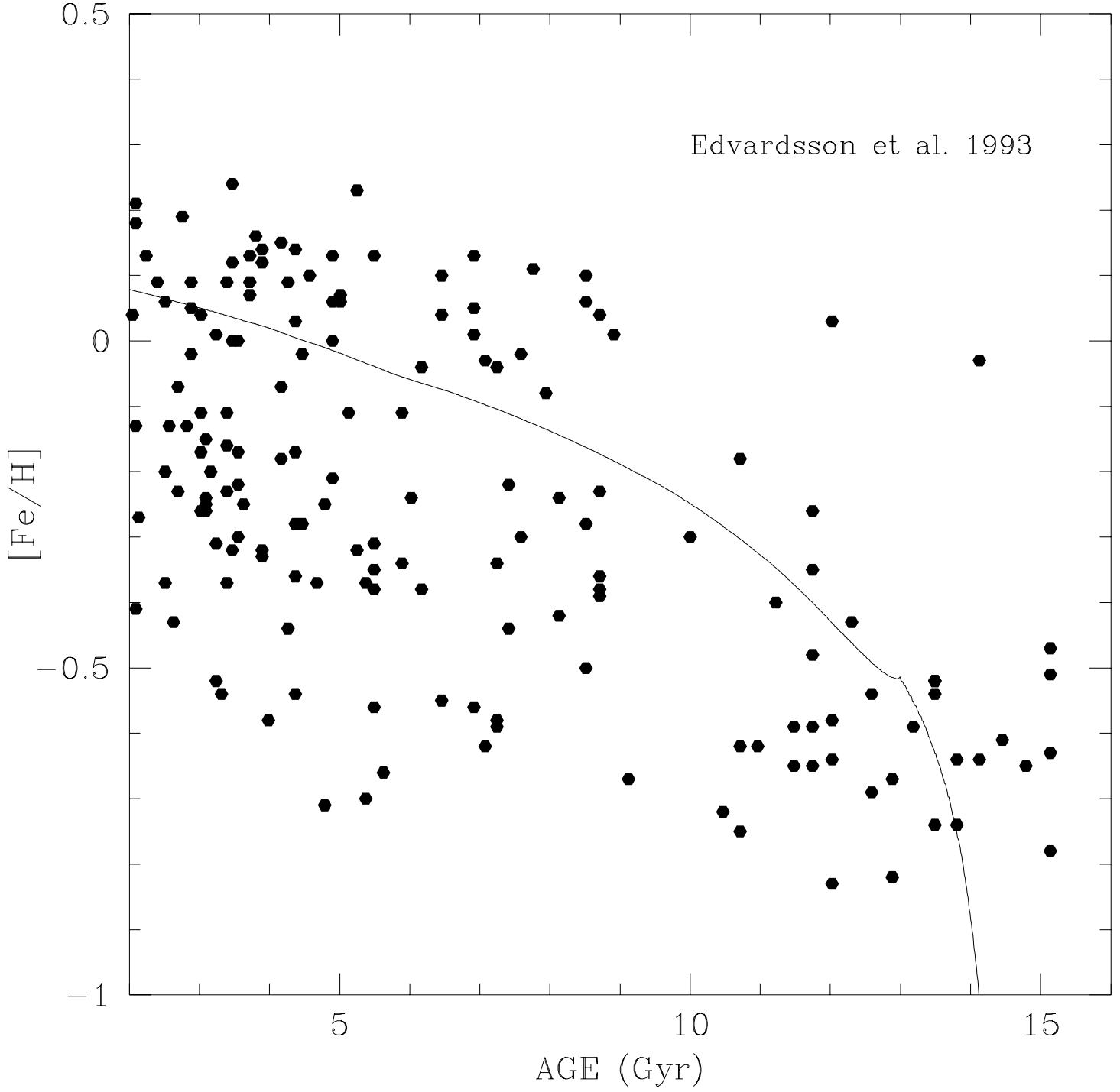


Fig. 1b.—

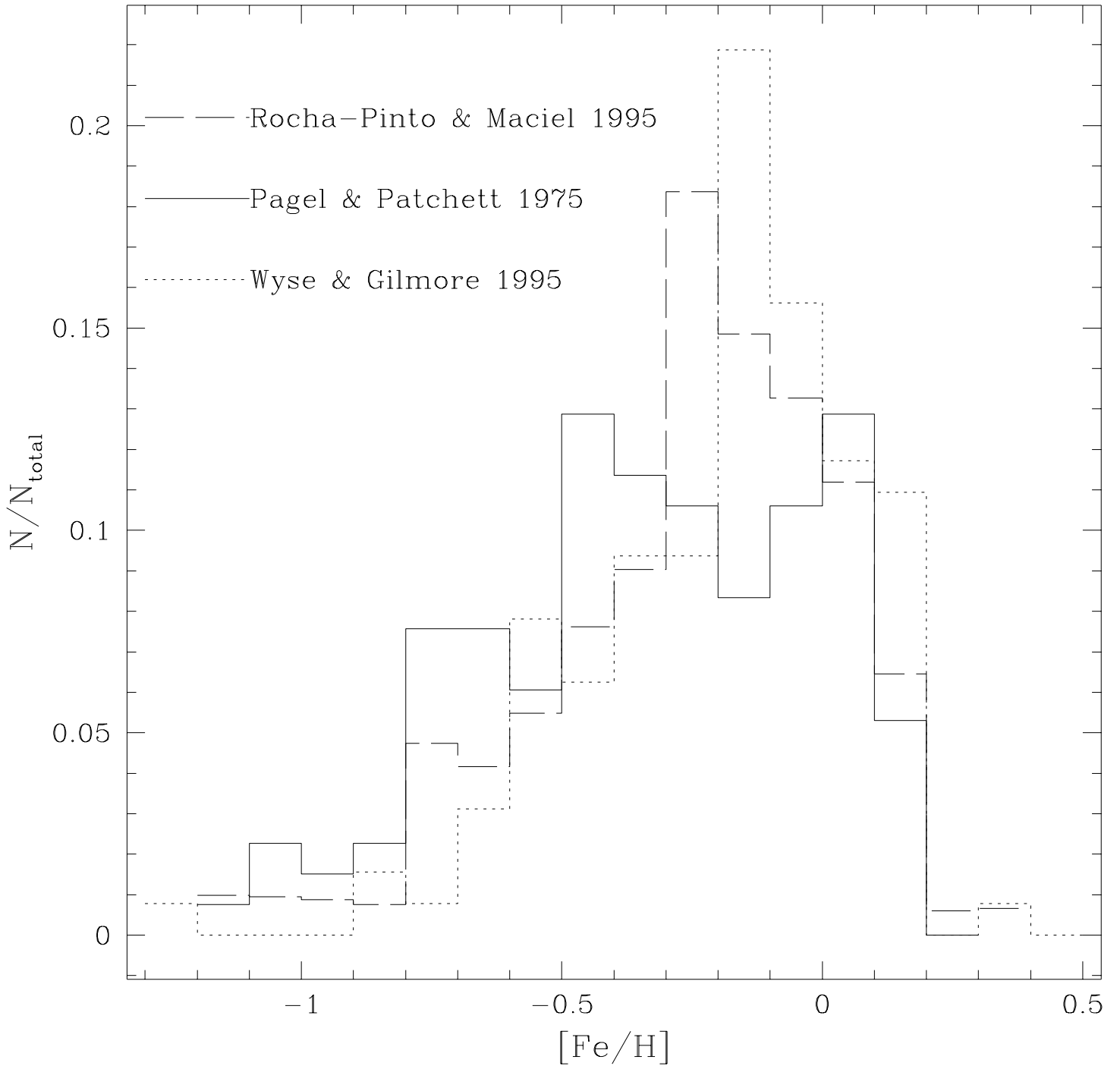


Fig. 2.—

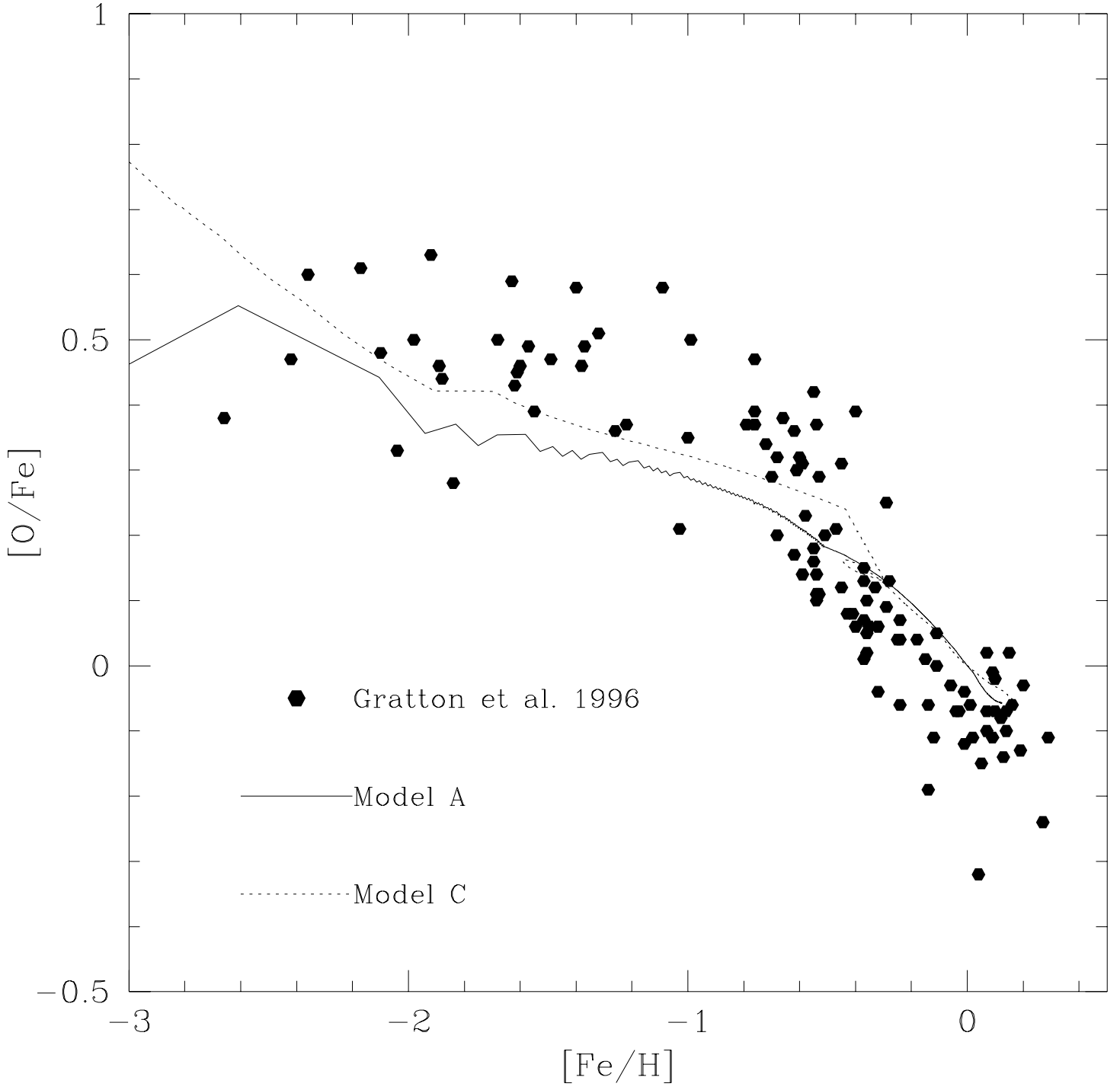


Fig. 3.—

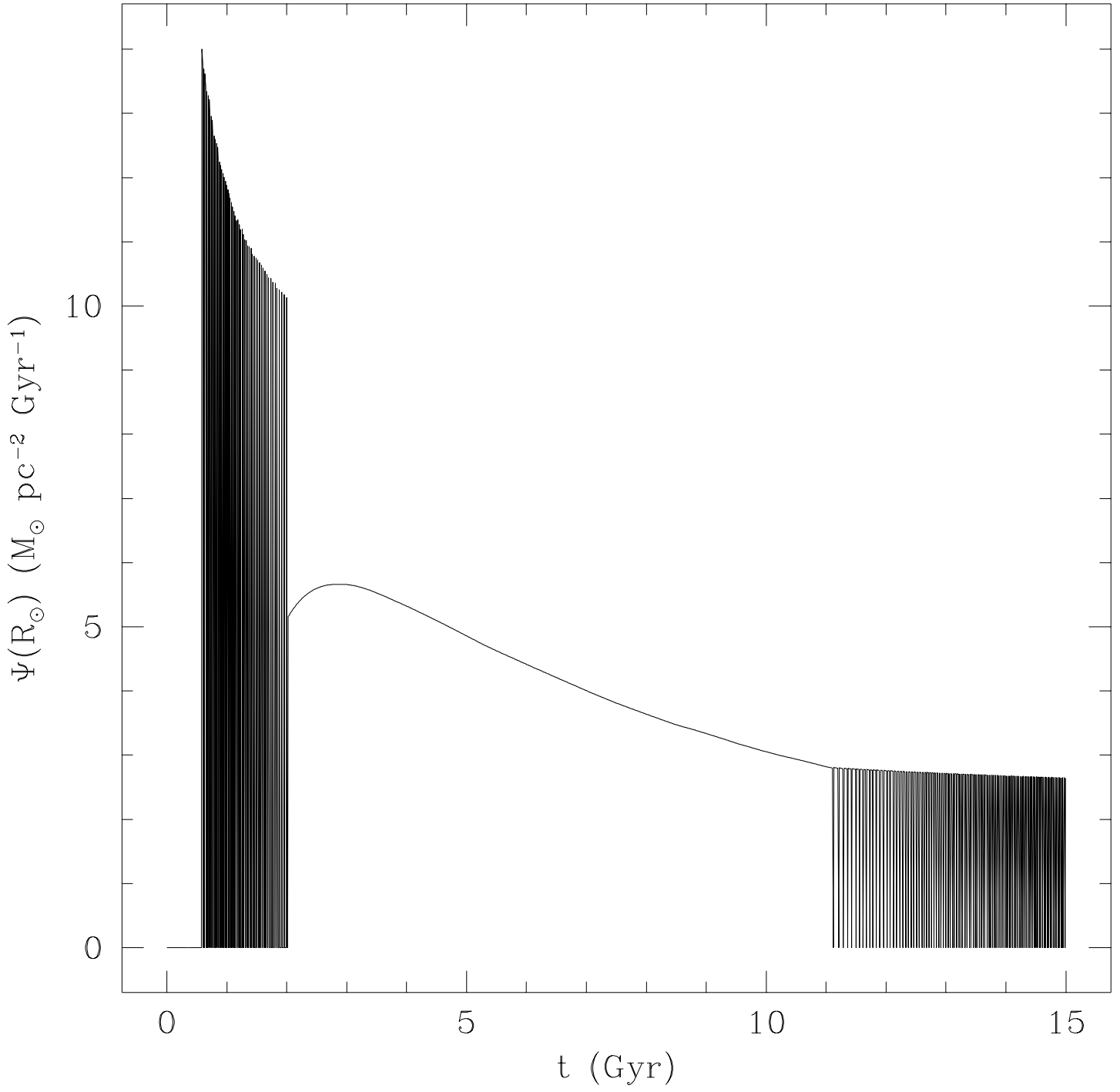


Fig. 4.—

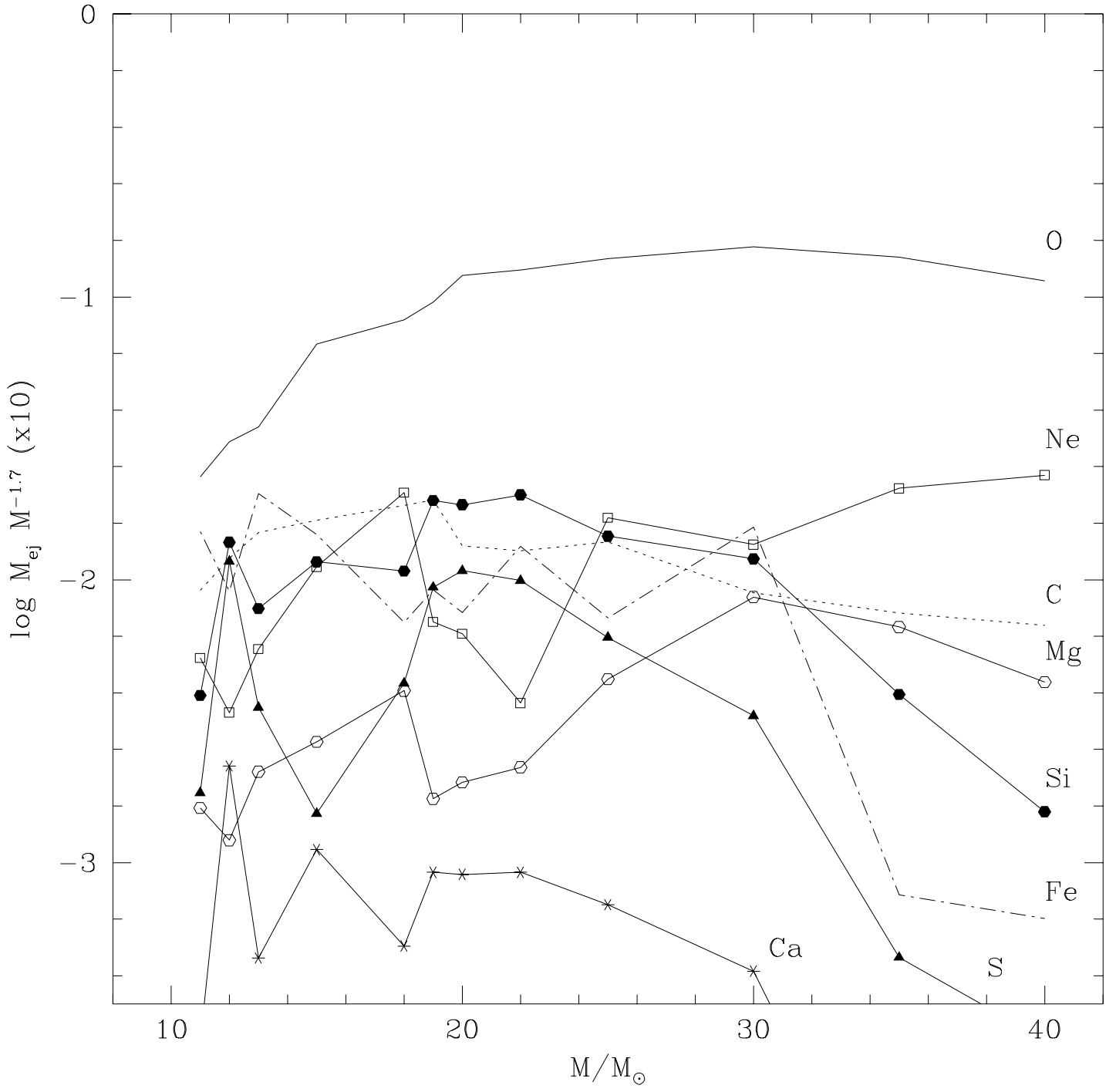


Fig. 5.—

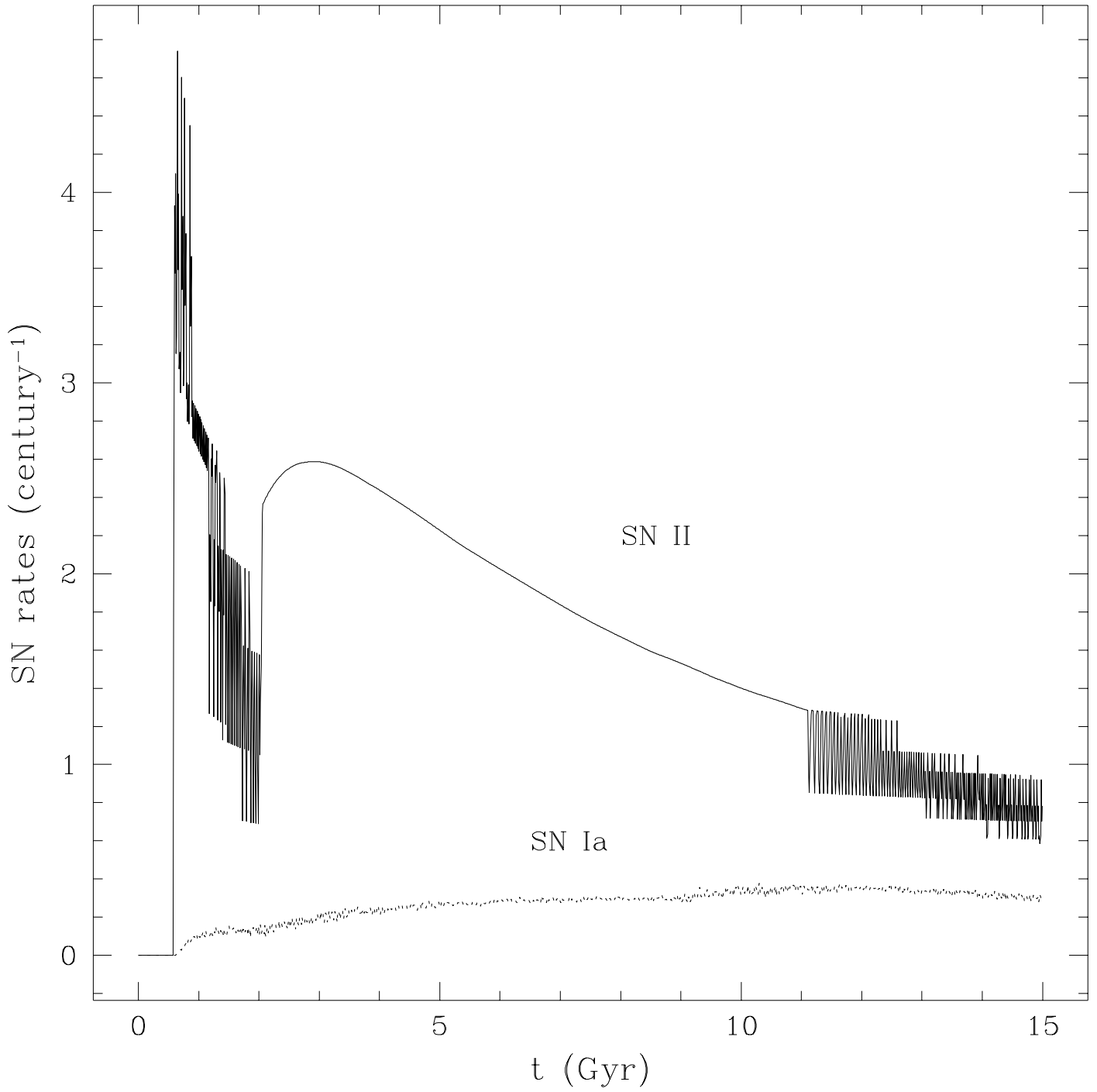


Fig. 6.—

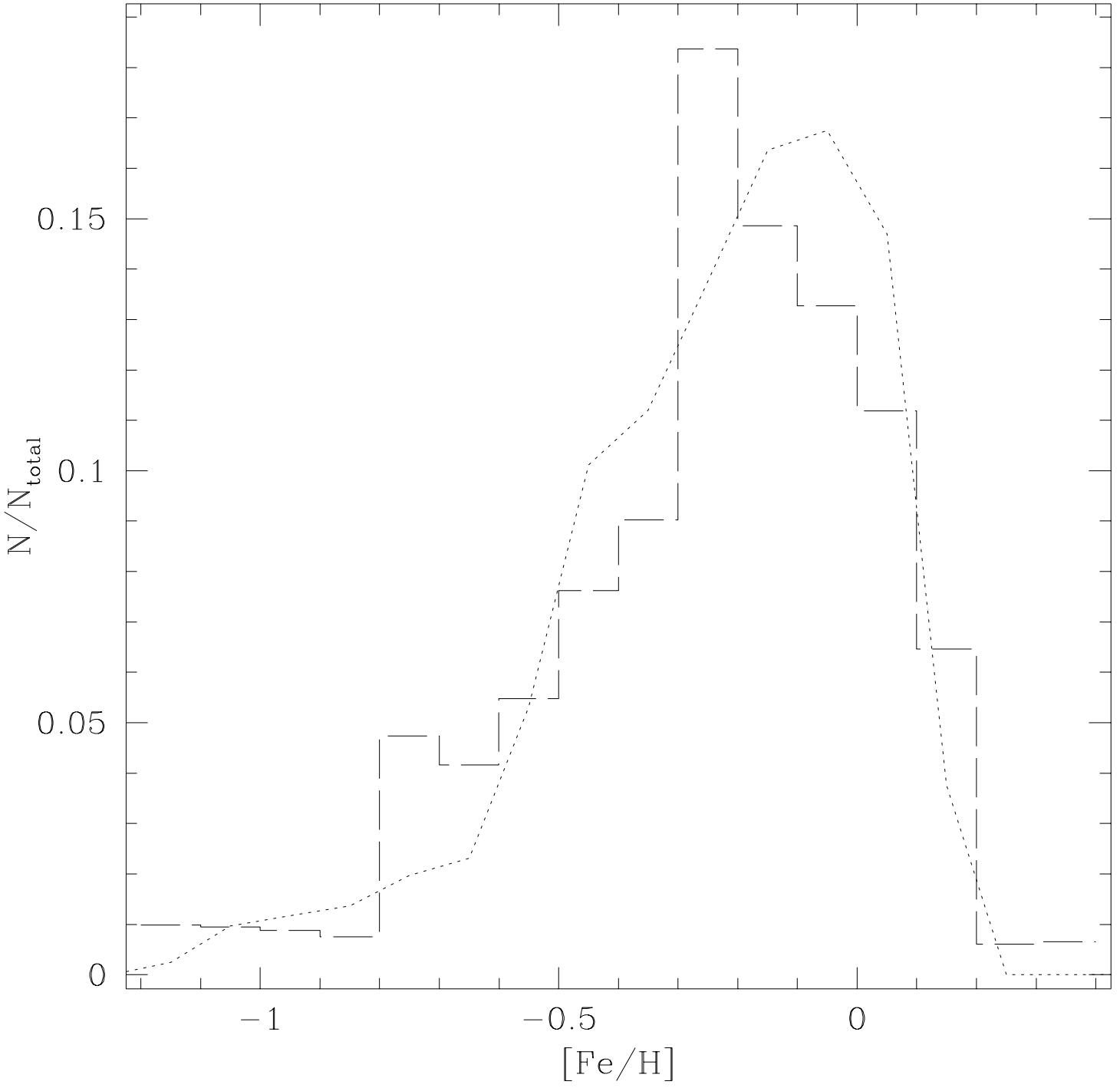


Fig. 7.—

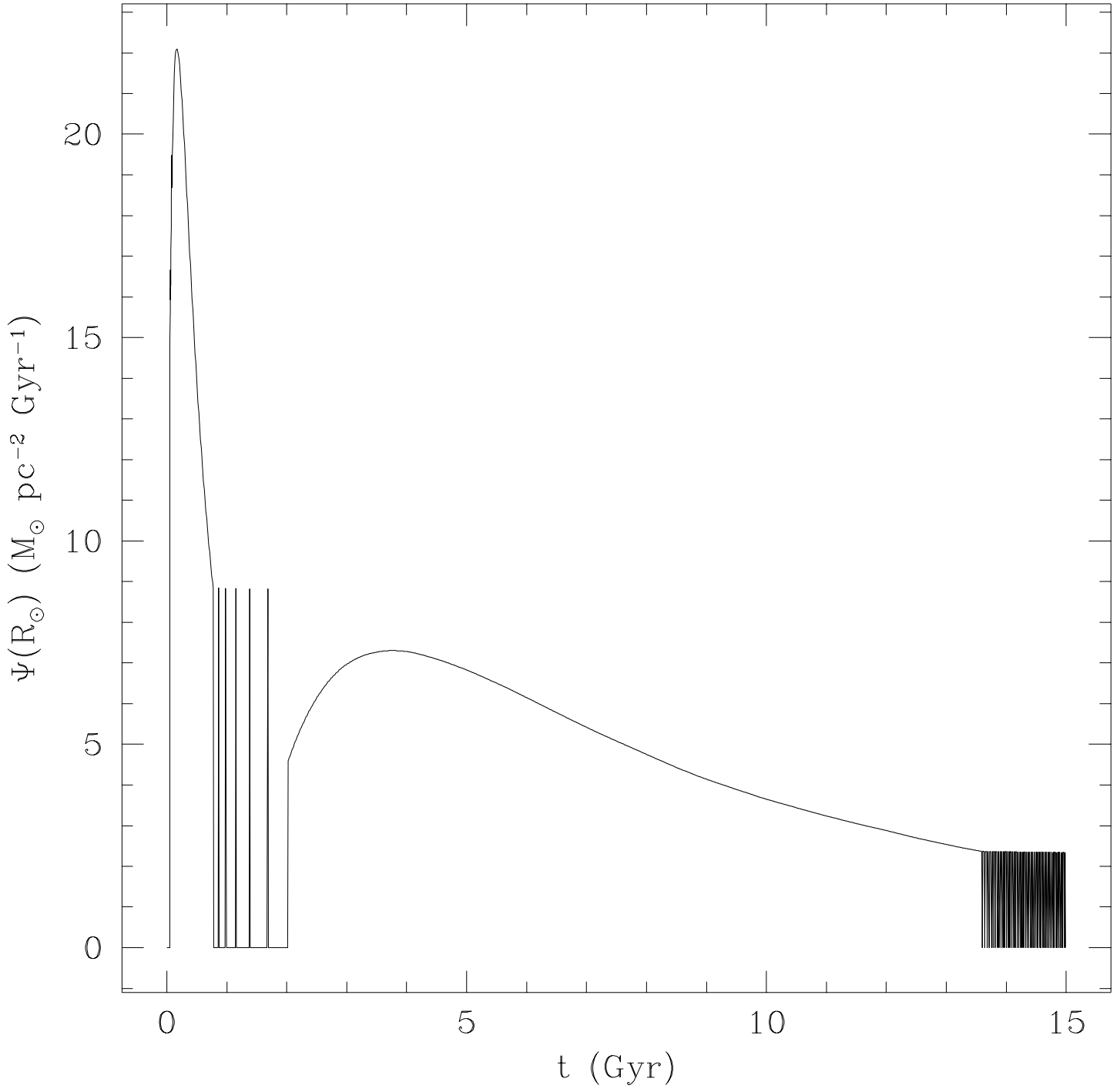


Fig. 8.—

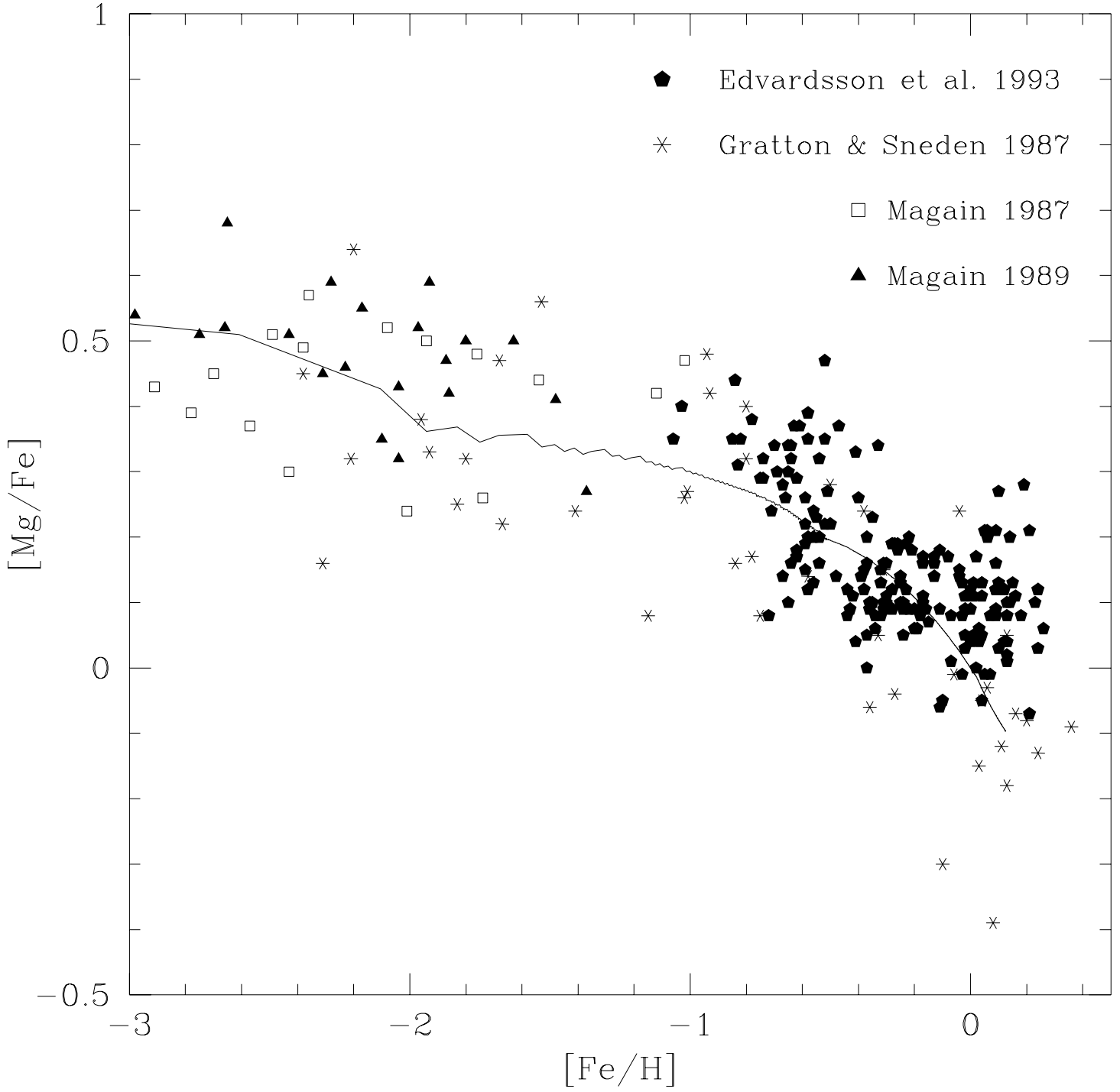


Fig. 9a.—

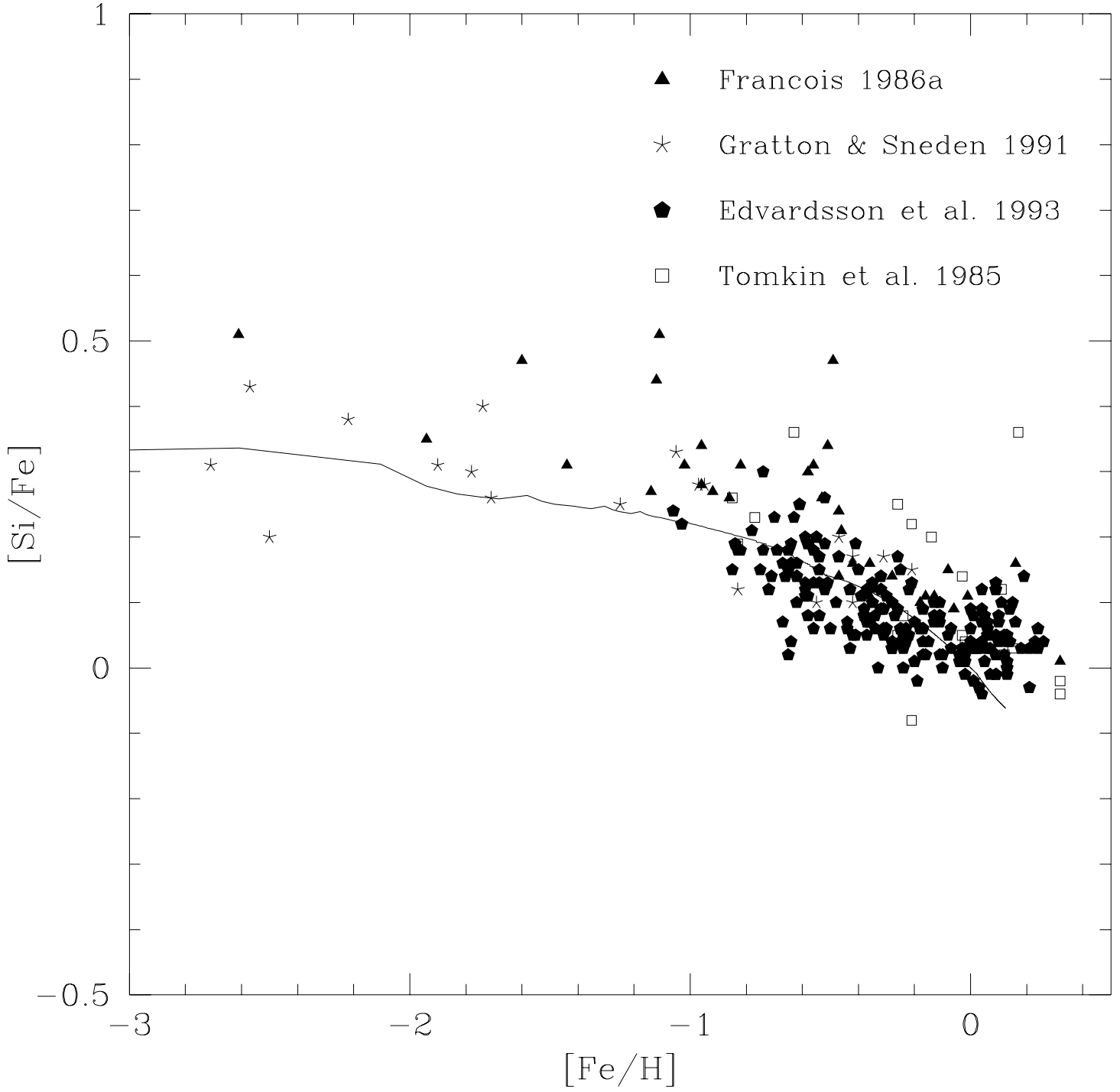


Fig. 9b.—

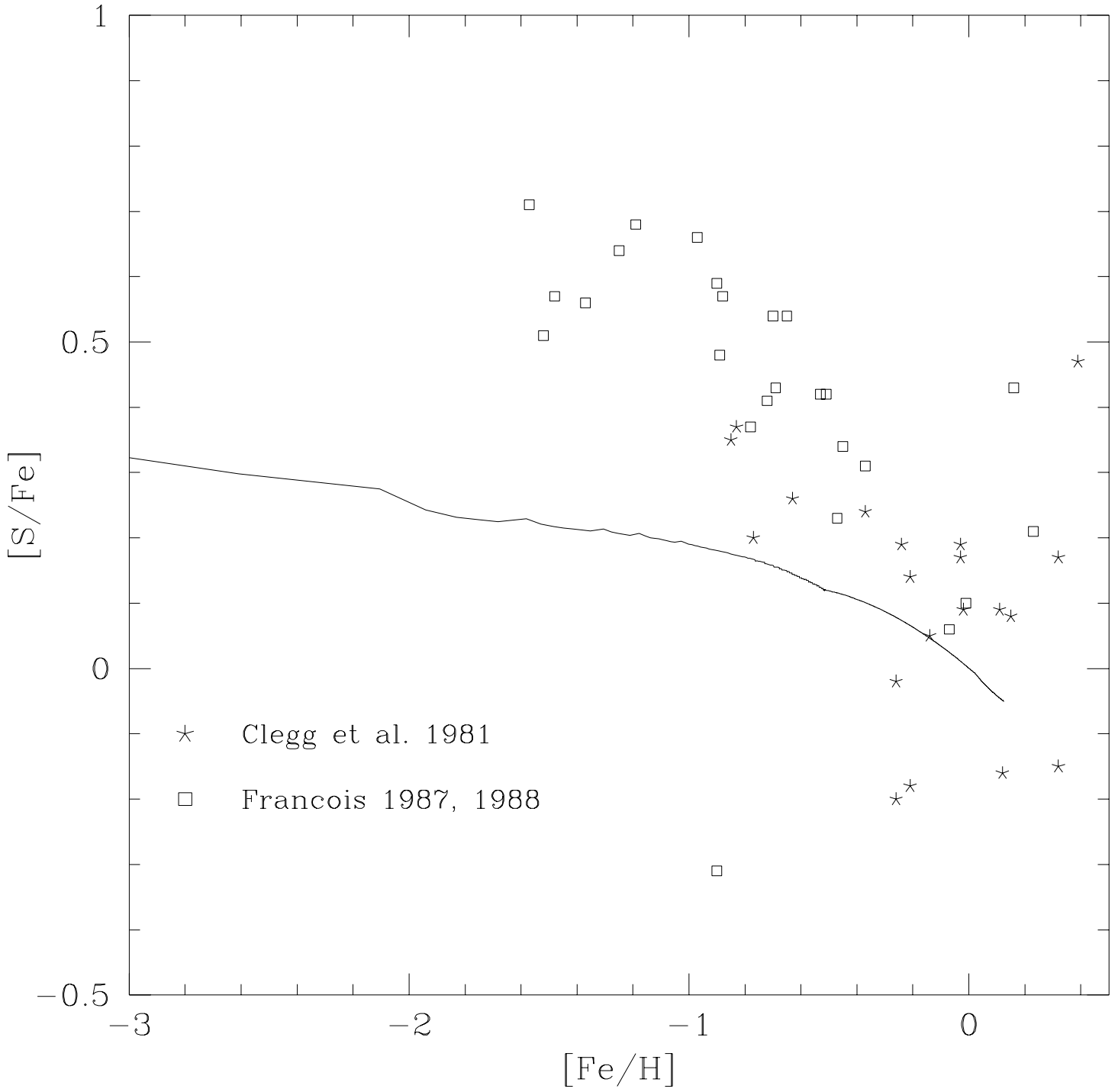


Fig. 9c.—

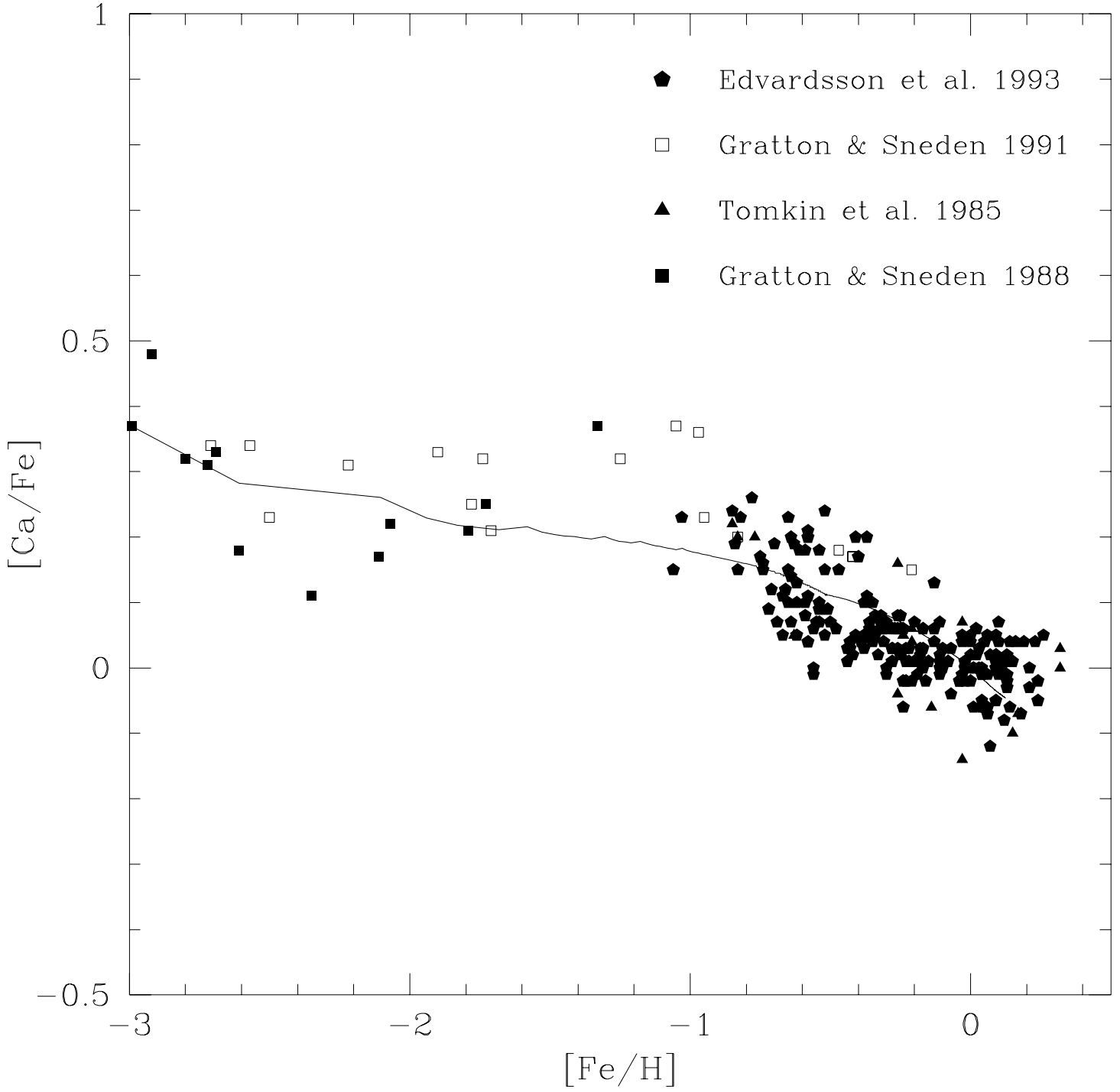


Fig. 9d.—

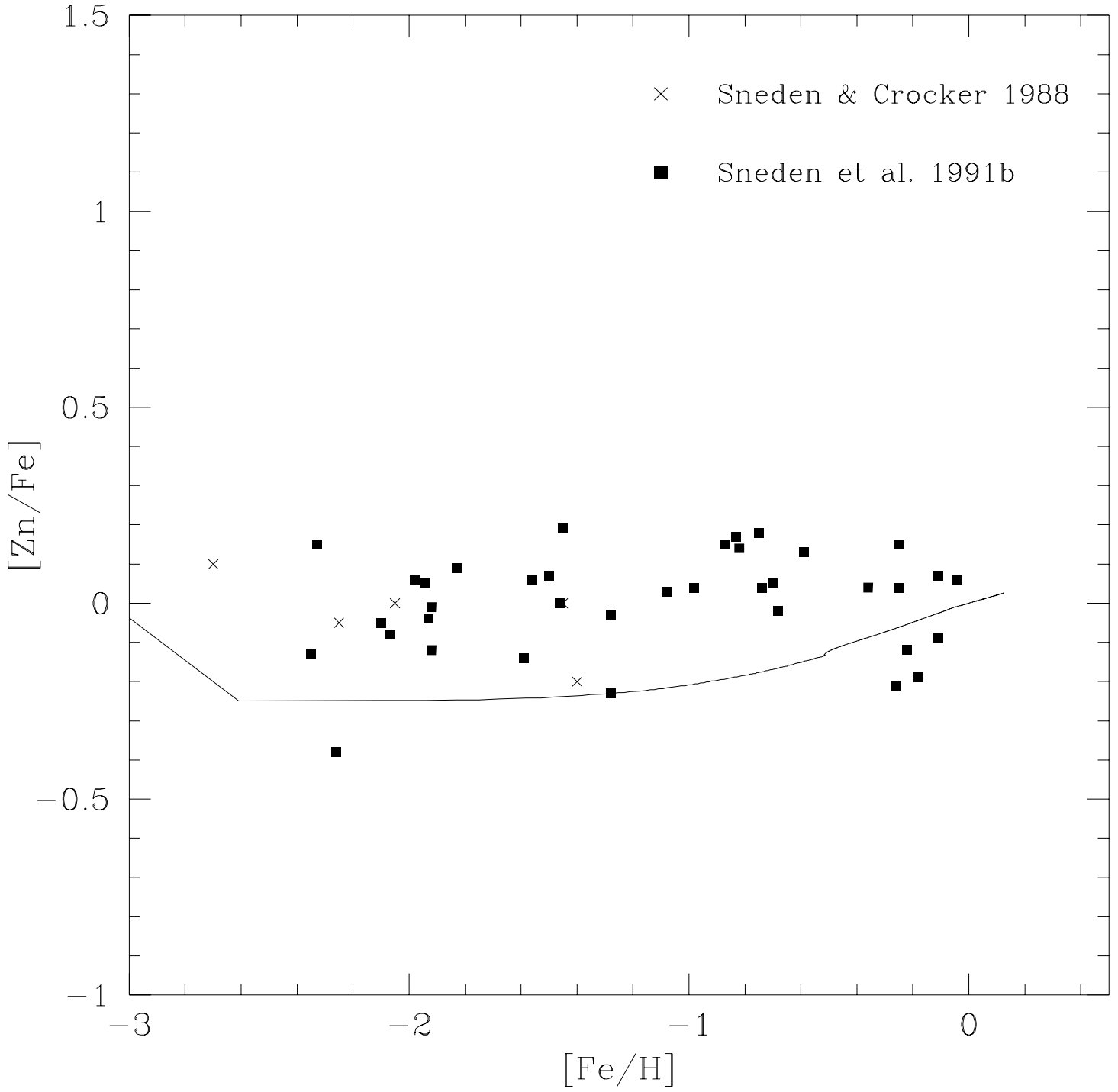


Fig. 10a.—

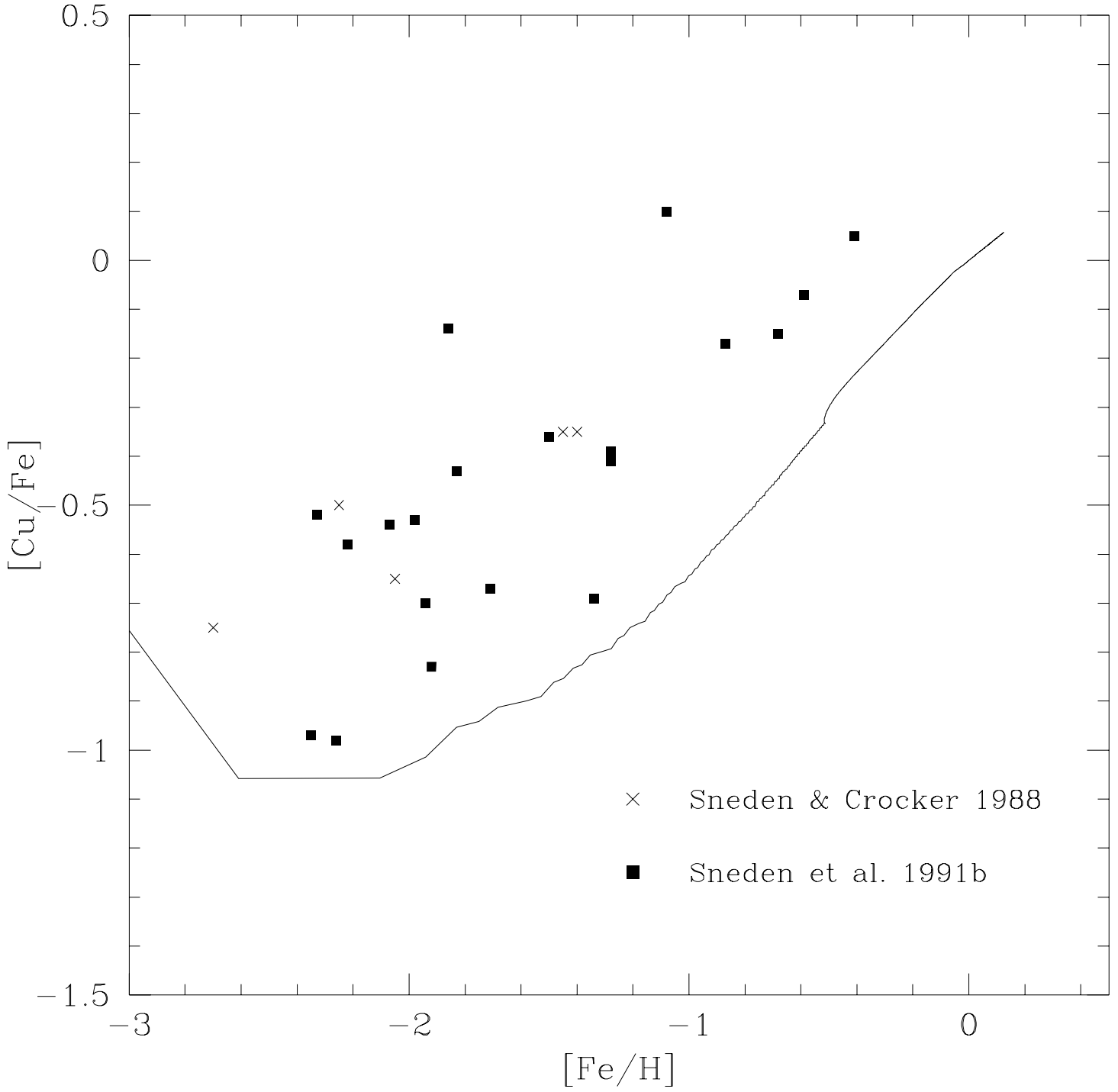


Fig. 10b.—

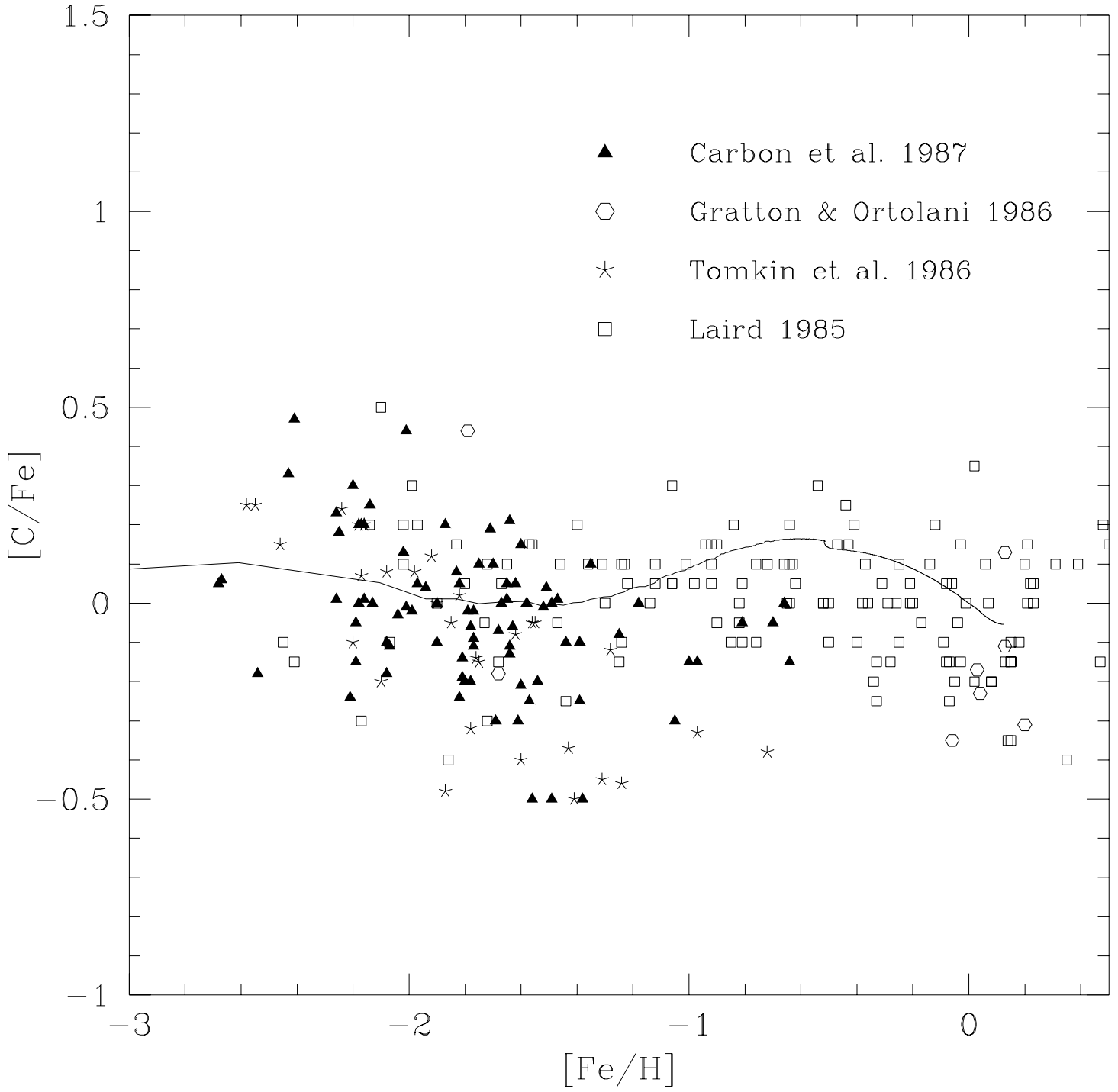


Fig. 11.—

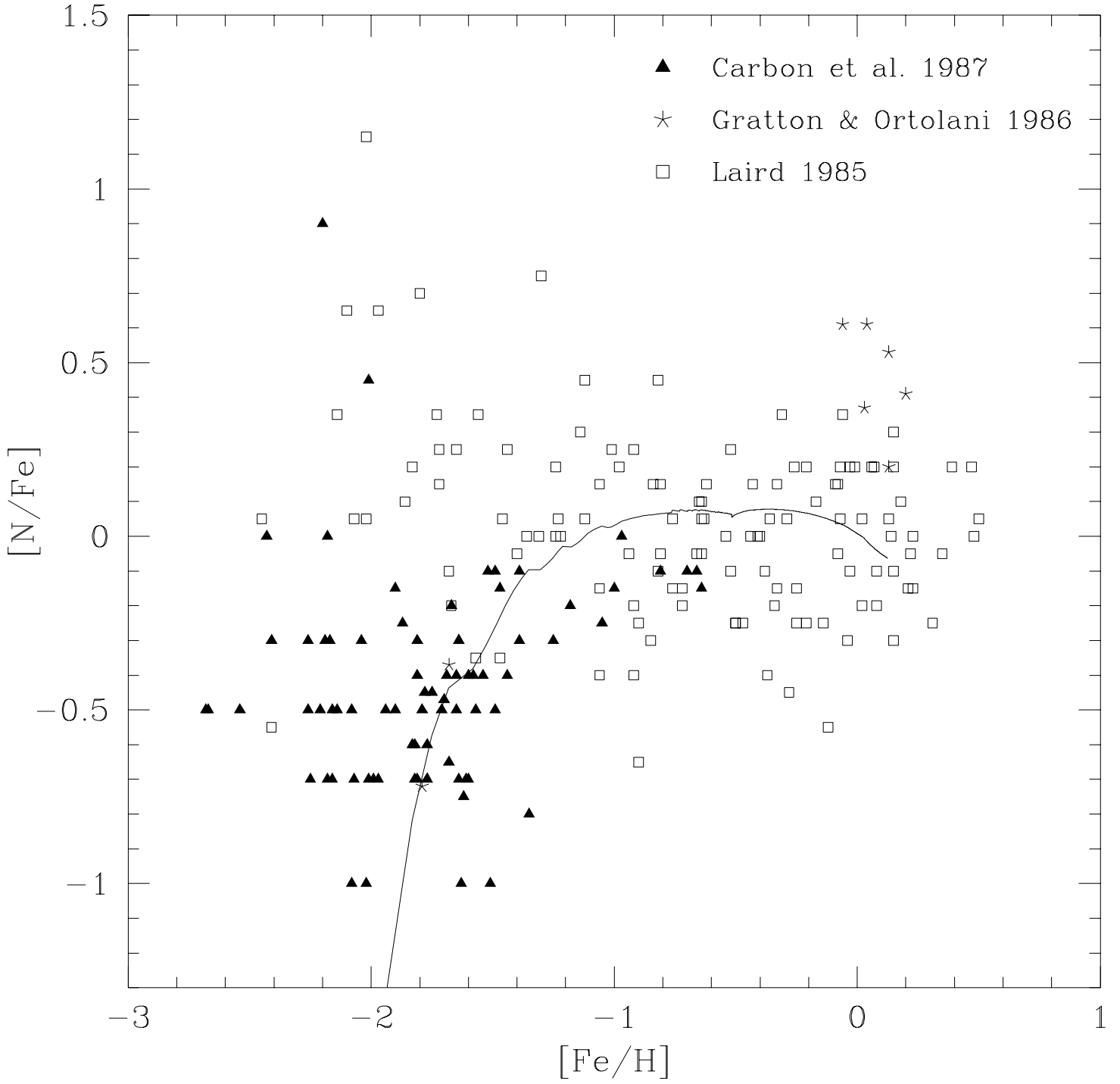


Fig. 12.—

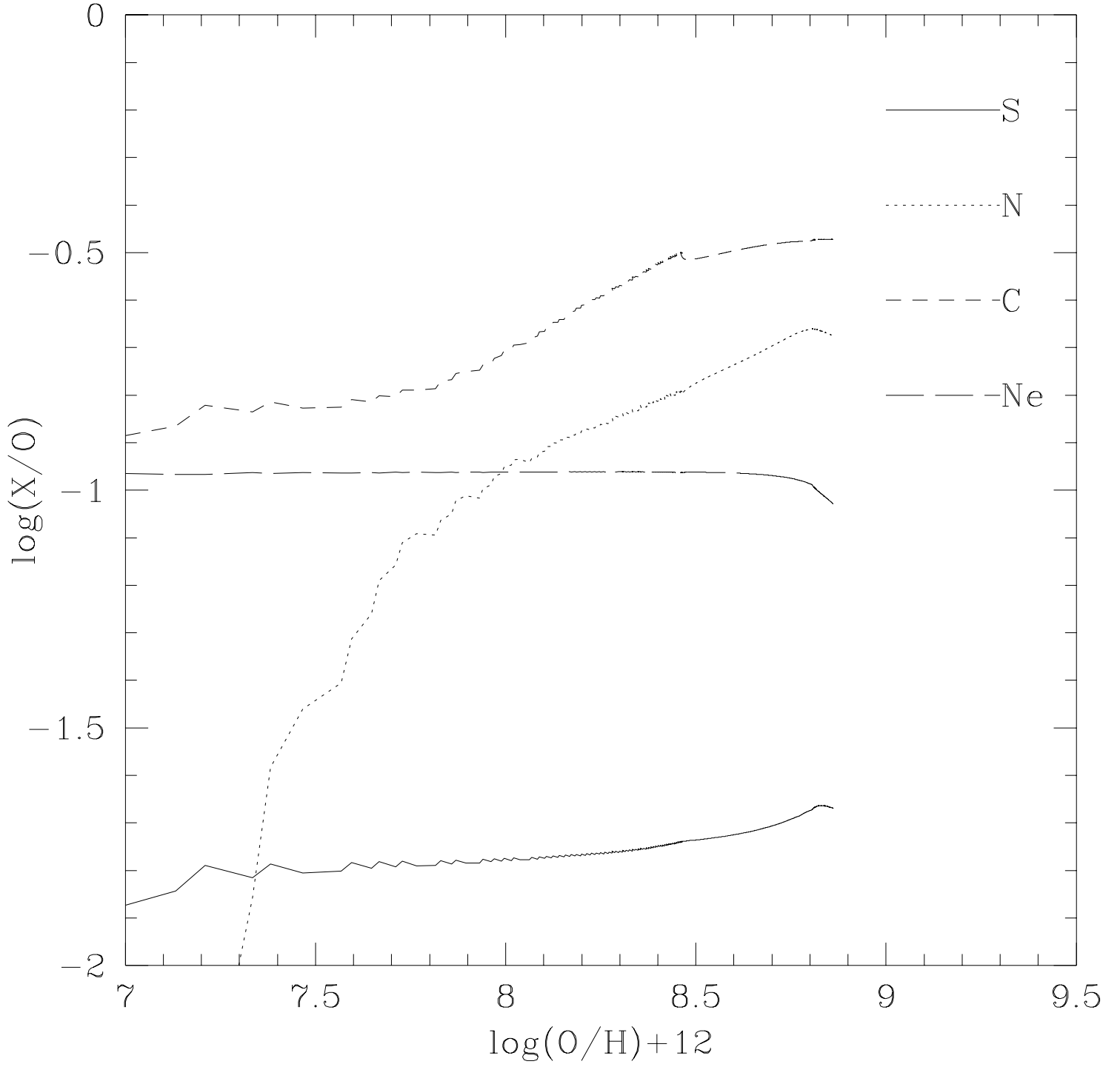


Fig. 13.—

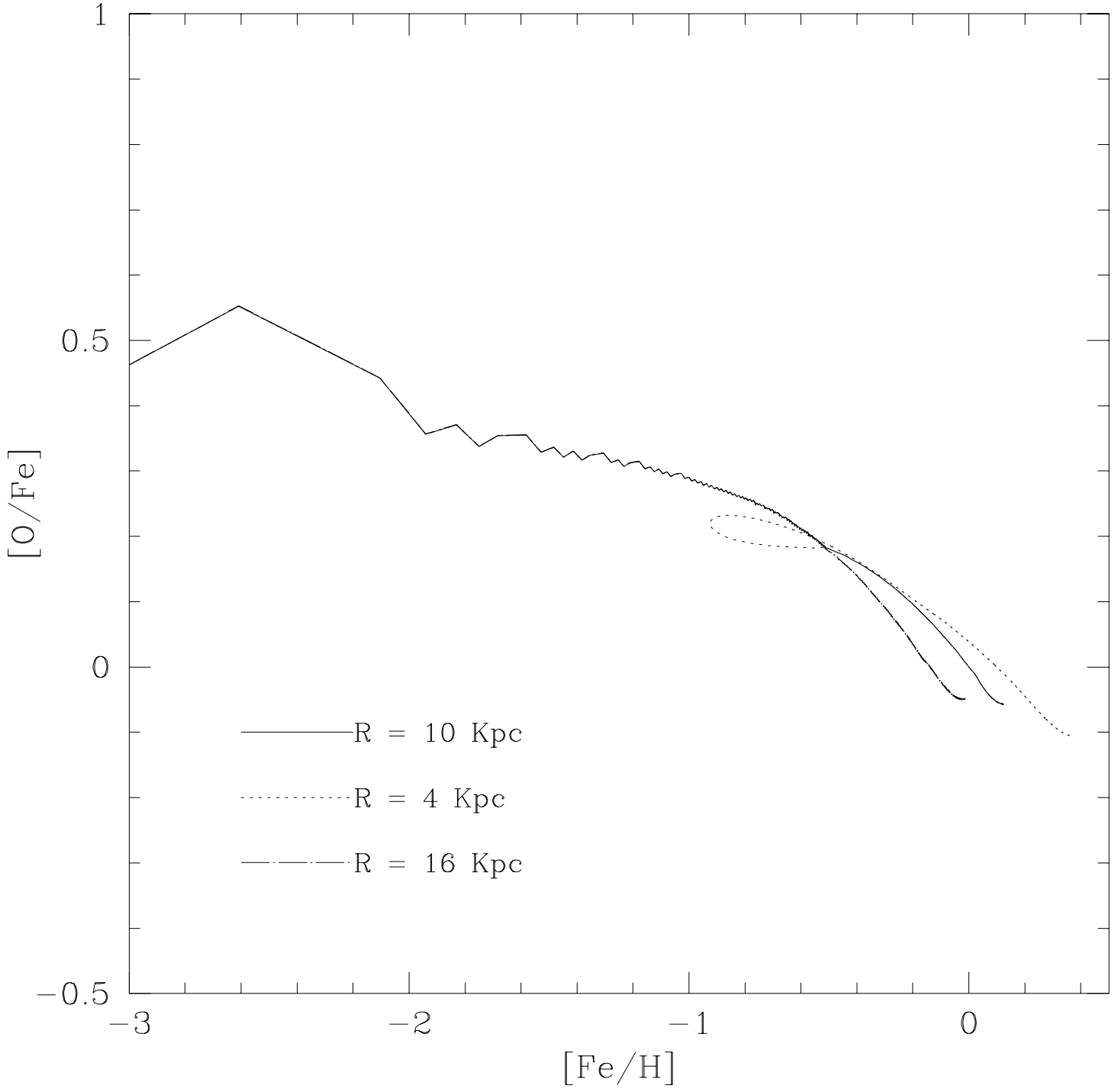


Fig. 14.—

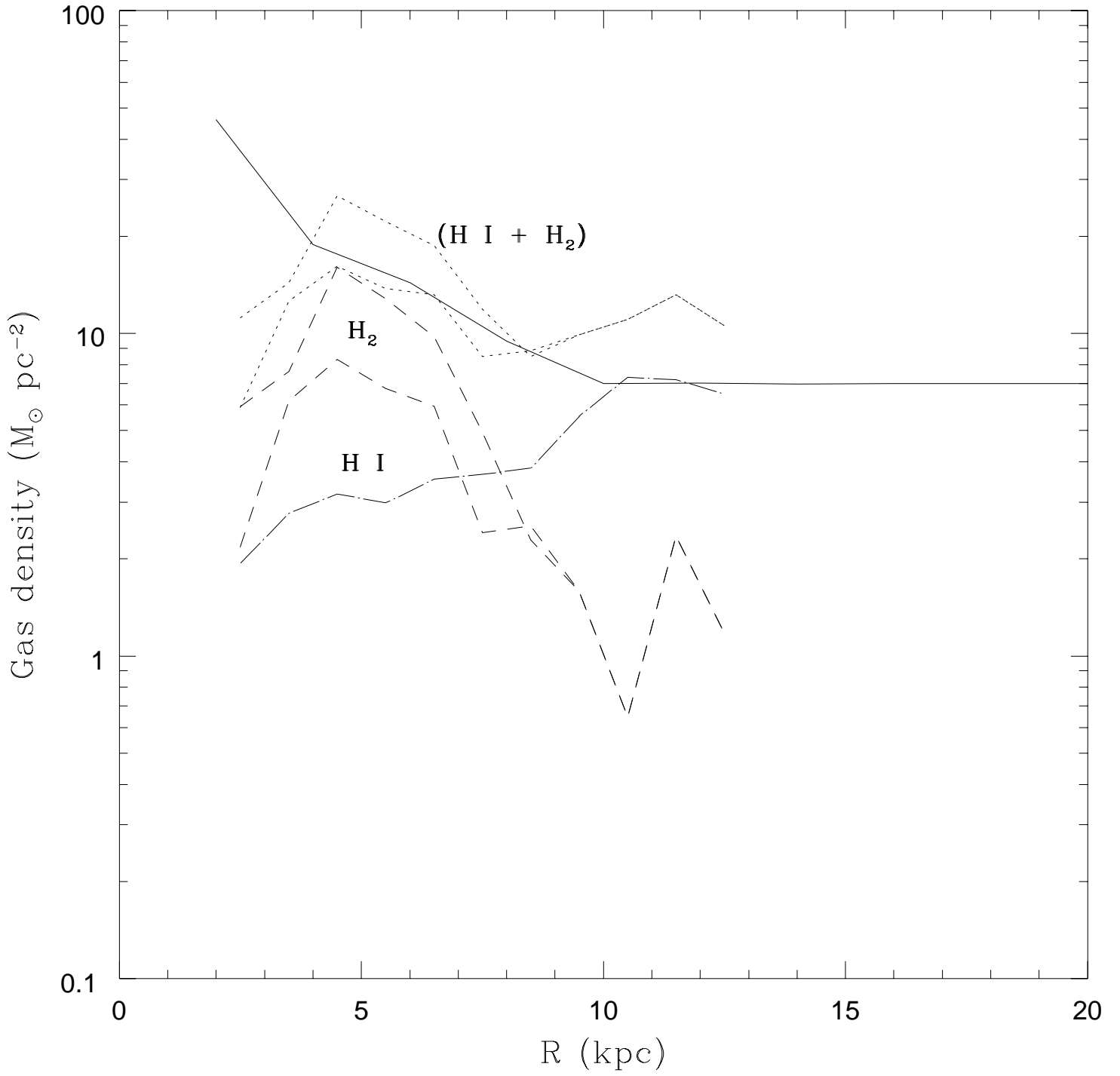


Fig. 15.—